

CROSS-TEST COMPARISONS AND REYNOLDS NUMBER EFFECTS IN THE CRM-HL ECOSYSTEM

Courtney S. Winski[1], Melissa Rivers[1] & Seyedeh Sheida Hosseini[2]

[1]NASA Langley Research Center, Hampton, VA, USA
[2]NASA Ames Research Center, Moffett Field, CA USA

Abstract

The High Lift Common Research Model (CRM-HL) ecosystem was created to address a critical challenge in aerodynamics: achieving certification-level confidence in predicting maximum lift coefficient ($C_{L_{Max}}$) under high-lift conditions. Current Computational Fluid Dynamics (CFD) tools struggle to accurately capture complex physics phenomena such as boundary layer transition, turbulence interactions, and Reynolds number effects. To overcome these limitations, the CRM-HL ecosystem integrates high-fidelity wind tunnel data with advanced computational methods, enabling rigorous validation and model calibration. This paper summarizes the evolution of the CRM-HL ecosystem, details global wind tunnel campaigns, and presents cross-test comparisons that quantify Reynolds number influences and geometric sensitivities. These efforts provide a robust foundation for turbulence and transition model development, accelerating progress toward simulation-driven certification.

Keywords: High-Lift, CFD, CRM-HL, Reynolds number, wind tunnel

1. High Lift Common Research Model (CRM-HL) Ecosystem Overview

The High Lift Common Research Model (CRM-HL) ecosystem was created to achieve certification-level confidence in predicting high-lift performance using computational methods. Accurate prediction of maximum lift coefficient ($C_{L_{Max}}$) and complex flow phenomena is critical for safer, more efficient aircraft and reducing costly physical tests.

1.1 Background

Aerodynamic research on high-lift systems has long been limited by restricted access to modern aircraft geometries. Proprietary constraints forced reliance on outdated models, slowing CFD validation under certification conditions. High-lift configurations—featuring slats, flaps, and fairings—introduce complex interactions, flow separation, and transition phenomena, demanding precise modeling and high-fidelity data. To close this gap, the aerospace community created the CRM-HL ecosystem, a global partnership offering standardized, open-access geometry and shared experimental data. This collaborative framework enables joint CFD validation and accelerates progress toward simulation-driven certification. The initial low-speed, high-lift configuration was defined in 2016 by Lacy and Sclafani [1] in 2016, based on the high-speed CRM model. The final reference configuration [2] was defined in 2020.

1.2 Ecosystem Development

The CRM-HL ecosystem was created to overcome limitations from proprietary data and fragmented research. It provides a standardized high-lift configuration based on a generic commercial transport geometry, developed by Boeing and NASA, and openly shared worldwide. Its modular, scalable design supports both semispan (SS) and full-span (FS) wind tunnel models, with interchangeable components—slats, flaps, nacelles, pylons, and fairings—enabling targeted aerodynamic studies without

building new models. Since 2019, CRM-HL has become an international benchmark, with coordinated campaigns at NASA and global facilities involving twelve official partners generating extensive datasets on forces, moments, pressures, and flow visualization. All data and geometry definitions are shared through NASA's CRM repository and workshops, creating one of the most comprehensive validation frameworks for reducing predictive uncertainty and advancing simulation-driven certification.

2. Global Wind Tunnel Campaigns

Wind tunnel testing is the foundation of the CRM-HL ecosystem, providing benchmark datasets for validating CFD under certification conditions. Coordinated campaigns across facilities and model scales isolate Reynolds number (RE) effects, geometric sensitivities, and tunnel influences, creating a cross-validated basis for turbulence and transition model calibration. Table 1 lists the currently built and tested CRM-HL ecosystem models, Table 2 lists the wind tunnels that have been used for CRM-HL ecosystem testing campaigns, and Table 3 shows a timeline of the completed CRM-HL ecosystem tests. The CRM-HL Ecosystem member data and models discussed herein are the German Aerospace Center (German: Deutsches Zentrum für Luft- und Raumfahrt e.V.) (DLR), the European Windtunnel (ETW), the Japan Aerospace Exploration Agency (JAXA), Kawasaki Heavy Industries, Ltd. (KHI), the National Aeronautics and Space Administration (NASA), and the French National Office for Aerospace Studies and Research (Office National d'Études et de Recherches Aérospatiales) (ONERA).

No data will be shown from the NASA 10%-scale CRM-HL test in QinetiQ 5-Metre (Q5m) since the NASA 10%-scale CRM-HL model outer mold line (OML) is a precursor to the final CRM-HL OML design geometry. Data from the NASA 5.2%-scale CRM-HL High RE test in NTF and data from the NASA 2.7%-scale CRM-HL High RE Icing Experimental Database (ICED) CRM test in ETW are still preliminary as final data corrections have not yet been applied. This paper does not include data from the JAXA 8%-scale CRM-HL test in JLWT or from the ONERA 5.1%-scale High Lift Large Reference Model (LRM-HL) Icing test in QinetiQ 5-Metre, as those data sets have not yet been officially released.

Table 1 – CRM-HL Wind Tunnel Models

Name	Scale	Owner	Span
KHI 3.23%-scale FS	3.23%	KHI	full-span (FS)
JAXA 8%-scale SS	8%	JAXA	semispan (SS)
NASA 2.7%-scale FS	2.7%	NASA	FS & SS
NASA 5.2%-scale SS	5.2%	NASA	SS
NASA 10%-scale SS[1]	10%	NASA	SS
ONERA 5.1%-scale FS	5.1%	ONERA	FS

[1] The NASA 10%-scale CRM-HL is a precursor to the final CRM-HL design geometry.

Table 2 – Wind Tunnels Used for CRM-HL Tests

Name	Abbreviation	Location
3 x 3m Kawasaki Low-Speed Aero-Acoustic Wind Tunnel	KLWT	Gifu, Japan
European Transonic Windtunnel	ETW	Cologne, Germany
JAXA 6.5m x 5.5m Low-Speed Wind Tunnel	JLWT	Chofu, Tokyo, Japan
Low-Speed Wind Tunnel at Braunschweig (DNW)	NWB	Braunschweig, Germany
NASA 14- by 22-Foot Subsonic Tunnel	14x22	Hampton, VA, USA
National Transonic Facility (NASA)	NTF	Hampton, VA, USA
ONERA F1 Pressurized Low-Speed Wind Tunnel	F1	Toulouse, France
QinetiQ 5-Metre Low-Speed Wind Tunnel	Q5m	Farnborough, UK

Table 3 – CRM-HL Wind Tunnel Tests

Year	Quarter	Description
2019	Q4	NASA 10%-scale CRM-HL[1]est in Q5m [3]
2022	Q1	ONERA 5.1%-scale LRM-HL test in F1 [4] [5]
2022	Q3	NASA 5.2%-scale CRM-HL Model check out test in 14x22, T668 [6]
2023	Q1	KHI 3.23%-scale CRM-HL test in KLWT [7]
2023	Q1	ONERA 5.1%-scale LRM-HL test in F1 [4] [5]
2023	Q2	NASA 5.2%-scale CRM-HL test in NWB [8] [9]
2024	Q1	NASA 5.2%-scale CRM-HL High RE test in NTF, T237[2][10] [11] [12]
2024	Q3	NASA 5.2%-scale CRM-HL Flow Visualization test in 14x22, T682
2025	Q3	NASA 2.7%-scale CRM-HL Low Re test in NTF, T240
2025	Q4	JAXA 8%-scale CRM-HL test in JLWT
2026	Q1	NASA 2.7%-scale CRM-HL High RE ICED CRM test in ETW, T857[2][13]
2026	Q1	ONERA 5.1%-scale LRM-HL Icing test in Q5m

[1] The NASA 10%-scale CRM-HL is a precursor to the final CRM-HL design geometry.
[2] NASA 5.2%-scale semispan NTF Test 237 data and NASA 2.7%-scale full-span test in ETW data are PRELIMINARY.

2.1 QinetiQ 5-Metre Low-Speed Wind Tunnel (Q5m) Test of the NASA 10%-Scale Semispan Model, 2019

The QinetiQ 5-Metre Low-Speed Wind Tunnel entry in October and November of 2019 served as an early reference point for landing and takeoff configurations and helped shape the subsequent CRM-HL baseline. The Q5m is a pressurized, low-speed wind tunnel with a 5m W x 4.2m H x 12m L test section. The NASA 10%-scale CRM-HL model is a starboard-wing semispan model. It was designed and built after the initial low-speed configuration was defined by Lacy and Sclafani [1], based on the high-speed CRM model. Using NASA's 10%-scale SS model, the team collected forces, moments, and pressure distributions under repeatable conditions, while also investigating half model effects and facility differences; select results supported the AIAA High Lift Prediction Workshop #4 (HLPW4) [14]. Because the geometry predated final CRM-HL standardization, this dataset is not cataloged as official ecosystem data, yet it remains historically important for design iteration and for anchoring early CFD comparisons. The nacelle lip contour, the slat brackets and the strake, and the junction between the forward wing root and the fuselage were re-designed from the NASA 10%-scale model for the CRM-HL reference configuration. Testing details are available in Evans et al. [3]. Figure 1 shows the NASA 10%-scale CRM-HL model installed in the Q5m tunnel.

Early QinetiQ analyses highlighted the effects of the noted geometric deviations from the final CRM-HL reference configuration [2]. These insights, along with targeted studies (including wind tunnel floor blowing to examine boundary layer profile influences), provided practical guidance for subsequent campaigns and improved comparability across facilities. The Q5m tunnel is pressurized, and testing was conducted at Mach 0.20 (landing configuration (LDG)) and 0.26 (takeoff configuration (TO)), at chord Reynolds numbers (Re_C) of 3.3M (LDG), 4.0M (TO) and 5.49M (LDG).

2.2 ONERA F1 Pressurized Low-Speed Wind Tunnel Test of the ONERA 5.1%-Scale High Lift Large Reference Model (LRM-HL), 2022 & 2023

ONERA's pressurized F1 campaigns in March–April 2022 and February 2023 employed a 5.1%-scale full span High Lift Large Reference Model to examine Reynolds number sensitivity at elevated test section pressures, delivering high fidelity forces, pressures, and flow visualization in high lift regimes. ONERA's F1 tunnel, located in Toulouse, France is a pressurized tunnel, with a 4.5m W x 3.5m H x 11m L test section. Figure 2 shows a picture of the ONERA 5.1%-scale LRM-HL model installed in the F1.

At the time of ONERA's 5.1%-scale LRM-HL model design, the ecosystem definition did not yet specify standardized, detailed, geometry for slat and flap brackets or flap track fairings—only their number and spanwise positions. ONERA adapted bracket designs from HLPW4 geometry, resulting



Figure 1 – Picture of the NASA 10% CRM-HL model installed in Q5m [Photo: QinetiQ] [3].



Figure 2 – Picture of the ONERA 5.1% LRM-HL model installed in the F1 [Photo: ONERA] [5].

in minor deviations from the final CRM-HL baseline, for example, the wing under-slat surface (WUSS) positioning differs by 0.024 inches (0.6 mm), .0017 of the model chord (359.2mm chord), at the outboard section relative to the CRM-HL baseline geometry. The ONERA model high-lift system and nacelles, described in Lacy and Clark [2], were incorporated into the CRM-HL ecosystem geometry. The model was tested in the landing configuration at Mach 0.20, Re_C 1.6M, 3.0M, 3.8M, 5.0M, 5.8M and 5.9M, and testing details are available in Mouton et al. [4] [5]. The ONERA datasets strengthened cross facility comparisons and were leveraged in subsequent workshops (e.g., HLPW5).

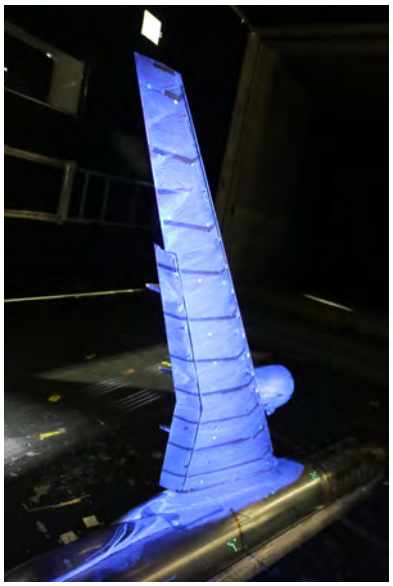
2.3 NASA 14- by 22-Foot Subsonic Tunnel (14x22) Model Check Out and Flow Visualizations Tests of the NASA 5.2%-Scale CRM-HL Semispan Model, 2022 & 2024

The NASA 5.2%-scale semispan model was tested in the NASA 14- by 22-Foot Subsonic Tunnel (14x22) in August and September of 2022 for a model checkout test to be sure that instrumentation in the model was working properly, all of the model parts fit together well, and model changes could be done smoothly as-designed while installed in a wind tunnel. The 14x22 tunnel, located in Hampton, VA, USA is a low-speed, atmospheric tunnel, with a 14.5ft W x 21.75ft H x 50ft L (4.4m W x 6.6m H x 18m L) test section. Force and moment and pressure data were collected during the test, providing the opportunity for tunnel-to-tunnel verification of the model, and for database supplementation for the NASA CRM-HL ecosystem. Eight configurations were tested at Mach 0.20, Re_C 1.55M (LDG) and Mach 0.26, Re_C 1.95M (TO), over an alpha range of -4° to +24°. The test is documented in Winski et al. [6]. Figure 3a shows a picture of the NASA 5.2%-scale SS model installed on the floor of the 14x22.

The NASA 5.2%-scale SS model was tested in the 14x22 a second time in September of 2024, focusing on collecting flow visualization data on the model using tufts and oil flow. The model was tested in the CRM-HL ecosystem baseline landing configuration (Landing - Nacelle, with nacelle on and no horizontal tail) for the entirety of this test campaign, at Mach 0.2, at an Re_C of 1.55M, from alpha -4° to 24°. The flow visualization data collected was openly shared, and has been used by NASA and the CRM-HL ecosystem to better understand the force and moment data collected on the same model during previous testing campaigns, however this paper will not cover any investigation of the flow visualization data. Figure 3b shows a picture from an oil flow run at $\alpha = 16.5^\circ$.



(a) NASA 5.2%-scale CRM-HL.



(b) Oil flow on the NASA 5.2%-scale CRM-HL.

Figure 3 – NASA 5.2%-scale CRM-HL SS model installed in the NASA Langley 14x22 [Photos: NASA].

2.4 3 x 3m Kawasaki Low-Speed Aero-Acoustic Wind Tunnel (KLWT) Test of the KHI 3.23%-Scale CRM-HL Full-Span Model, 2023

The Kawasaki Heavy Industries, Ltd. (KHI) 3.23%-scale full span campaign at the 3 x 3m Kawasaki Low-speed Aero-Acoustic Wind Tunnel (KLWT) provided a valuable mid-scale reference, closely aligned with the CRM-HL baseline while accommodating instrumentation needs. Pressure tubing routed from flaps and slats to the wing spar trough was housed by increasing bracket/fairing heights rather than widths, consistent with ecosystem guidance. A design level CAD comparison against the HLPW5 bare model found no differences, reinforcing the rigor of geometry control and offering a clean case for isolating instrumentation allowances in the height of the slat and flap brackets, from true aerodynamic effects. Figure 4 shows a picture of the KHI 3.23%-scale CRM-HL model installed in KLWT. Testing details are available in Hashioka et al. [7]. The KLWT, located in Gifu, Japan is a low-speed, atmospheric and acoustic tunnel, with a 3.0m W x 3.0m H x 9.0m L test section.



Figure 4 – Picture of the KHI 3.23% CRM-HL model installed in KLWT [Photo: KHI] [7].

The KHI model was tested in the landing and takeoff configurations in the KLWT. In the landing configuration the model was tested at Machs 0.10 , 0.20 , 0.23, 0.25, at Re_C 0.55M, 1.10M, 1.27M, 1.36M respectively. The KLWT dataset (forces and moments, pressures, and flow visualization with tufts and oil flow) expanded cross facility coverage and helped bridge ONERA's full span tests and NASA's semispan/full-span entries.

2.5 Low-Speed Wind Tunnel at Braunschweig (NWB) DLR Test of the NASA 5.2%-Scale Semispan CRM-HL Model, 2023

Under a NASA–DLR arrangement, the NASA 5.2%-scale SS CRM-HL model was tested in The German-Dutch Wind Tunnels' (DNW - Deutsch-Niederländische Windkanäle) Low-Speed Wind Tunnel at Braunschweig (NWB - Niedergeschwindigkeits-Windkanal Braunschweig) from May 9 to July 6, 2023, yielding forces, moments, and pressures for cross facility comparison at lower Reynolds numbers. The NWB, located in Braunschweig, Germany is a low-speed atmospheric and acoustic wind tunnel, with a 3.25m W x 2.8m H x 8.0m L test section. A picture of the NASA 5.2%-scale SS CRM-HL model installed in the NWB is shown in Figure 5. Testing details can be found in Puelm et al. [8] [9]. The test used a duplicated, but lighter weight, fuselage from the other tests of the NASA 5.2%-scale SS wing. The model was installed on the floor of the atmospheric wind tunnel.
Testing of the NASA 5.2%-scale SS model in the NWB was conducted at Mach numbers of 0.15, 0.2 and 0.23 at chord Reynolds numbers of 1.2M, 1.6M and 1.8M, respectively. DLR's broader work with the NASA hardware, including configurational variations such as an ultra high bypass nacelle [15] and alternative leading edge devices, further enriched the ecosystem's understanding of installation effects and instrumentation strategies, complementing NWB comparisons and informing future workshop datasets.



Figure 5 – NASA 5.2%-scale semispan CRM-HL model installed in the NWB Tunnel at DLR [Photo: DLR].

2.6 National Transonic Facility (NTF) High Reynolds Number Test of the NASA 5.2%-Scale Semispan CRM-HL Model, Cryogenic, 2024

The National Transonic Facility (NTF) campaign with NASA's 5.2%-scale SS model, from January 3 to May 23, 2024, achieved flight level Reynolds numbers using cryogenic operation, producing a benchmark dataset for certification level analysis. The entry spanned Mach 0.20–0.35 and chord Reynolds numbers from 1.61M to 30M, with 85 runs and 32 repeats to strengthen statistical confidence and procedural cross checks. The NTF located in Hampton, VA, USA is a transonic, pressurized cryogenic wind tunnel, with a 8.2ft W x 8.2ft H x 25ft L (2.5m W x 2.5m H x 7.6m L) test section. In situ geometric validation using a Hexagon Absolute Arm confirmed tight as-built tolerances relative to the as-designed CAD, bolstering the credibility of pressure and load measurements across landing, takeoff, and iced configurations [10]. This campaign was designed to generate flight-representative aerodynamic data for the open CRM-HL ecosystem, supporting validation of CFD methods under certification-relevant conditions. A key objective was to acquire force and moment measurements for baseline and iced configurations, as detailed in Broeren et al. [16]. The port wing semispan model, developed by NASA as described in Ertsgaard and Winski [17], is shown installed on the NTF test section wall in Figure 6. These NTF data now serve as primary anchors for Large Eddy Simulation and Wall-Modeled Large Eddy Simulation (LES/WMLES) CFD investigations and reduced order modeling near $C_{L_{Max}}$.

2.7 National Transonic Facility Air Phase Test of the NASA 2.7%-Scale Full-Span CRM-HL Model, Test 240, 2025

To deepen cross scale insight and broaden configuration coverage, NASA executed NTF Test 240 using a 2.7%-scale FS CRM-HL model, structured around baseline landing plus multiple icing scenarios. The test took place from August 26, 2025 through September 5, 2025. Because of the small model size the lofted trailing edge CAD configuration was used in the design [18], and the slat and flap brackets were increased in height, not width, following the ecosystem standard, to accommodate pressure tubing. The campaign documented Mach 0.20, angles of attack from -4° to 22°, and systematic in test repeat runs, enabling Reynolds effect mapping between Re_C 1.1M and 5.49M in an air environment while maintaining a consistent measurement suite for forces and moments, static and dynamic pressures, wing deformation, and transition detection via integrated taps. Design and instrumentation followed ecosystem modularity: slat and flap angles adjustable, Kulite sensors distributed for redundancy and resolution, nacelle on or off and nacelle chine positions configurable, and hori-



Figure 6 – Picture of the NASA 5.2%-scale CRM-HL semispan model installed in the NTF [Photo: NASA].

zontal tail and landing gear states toggled to isolate component contributions. Model design details are available in Ertsgaard and Winski [19]. Figure 7 shows the NASA 2.7%-scale model installed in the NTF.



Figure 7 – NASA 2.7%-scale full-span CRM-HL model installed in the NTF [Photo: NASA].

The test matrix embedded comparison points against other ecosystem campaigns— KLWT KHI 3.23%-scale (Re_C 1.1M), NASA 5.2%-scale in NWB and 14x22 (Re_C 1.6M), JAXA 8%-scale (Re_C 2.6M), NTF 5.2%-scale SS, ONERA 5.1%-scale LRM-HL in F1 (Re_C 1.6M and 3.33M), and QinetiQ 10%-scale in Q5m (Re_C 3.33M and 5.49M), enabling structured normalization across facilities and scales. By pairing an air phase entry in 2025 with a planned cryogenic entry in 2027, the ecosystem will extend the Reynolds envelope for full span configurations and provides direct evidence of icing impacts on $C_{L_{Max}}$, drag rise, and pitching moment behavior near stall, further strengthening simulation driven certification workflows.

2.8 European Transonic Windtunnel (ETW) High Reynolds Number ICED CRM Test of the NASA 2.7%-Scale CRM-HL Full-Span Model, T857, 2026

The NASA 2.7%-scale CRM-HL full span model was tested at the European Transonic Windtunnel in Cologne, Germany, from April 8 to 24, 2026. The ETW, located in Cologne, Germany is a transonic,

pressurized, cryogenic wind tunnel, with a 2.4m W x 2.0m H x 9.0m L test section. The test focused on developing a high Reynolds number dry air icing database, including clean, no-ice runs on the landing configuration with nacelle and horizontal tail (HTail) installed. Testing details are available in Prince et al. [13]. 171 data runs were collected with 81 of those runs being repeats. The testing matrix included Reynolds number trends from Re_C 1.6M to 16M, and Mach trends (Mach 0.18 - 0.35), flow angularity, hysteresis, forces and moments, pressures, model deformation and Kulite data collection. Figure 8 shows the NASA 2.7%-scale full span CRM-HL model installed in ETW. Clean testing of the NASA 2.7%-scale CRM-HL full span model in ETW provided high Reynolds number data for the high lift ecosystem as well as the opportunity for tunnel-to-tunnel comparisons of the NASA 2.7%-scale model using the same model, the same upper swept strut and a sister balance to the one tested previously in NTF.

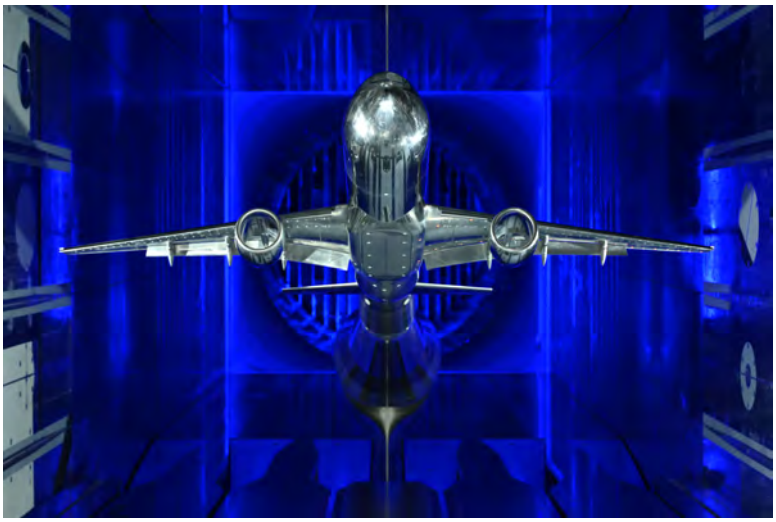


Figure 8 – Picture of the NASA 2.7%-scale CRM-HL full span model installed in the ETW [Photo: ETW].

2.9 Cross-Campaign Significance and Data Use

Collectively, these campaigns establish a multi-facility, multi-scale benchmark for high-lift aerodynamics: they quantify Reynolds number influence; expose sensitivities to bracket/fairing implementation under instrumentation constraints; and supply the open datasets needed to calibrate turbulence/transition models and improve predictive fidelity near $C_{L_{Max}}$. Results feed directly into AIAA High Lift Prediction Workshops, NASA's CRM repositories, and ecosystem partners' validation workflows, driving convergence toward robust, simulation driven certification. Table 4 notes the cross-campaign significance and notable findings for the CRM-HL ecosystem testing campaigns.

At matched chord Reynolds numbers, ONERA's full span results tended to produce a higher $C_{L_{Max}}$ than NASA's semispan tests and NASA's full-span tests, underscoring sensitivities to bracket/sealing implementation, localized geometry (e.g., WUSS), model mounting and spanwise support effect, which are key considerations when calibrating CFD near stall. At Re_C 1.1M KHI's full-span C_L is comparable to the NASA 2.7%-scale full-span model. KHI strengthened normalization efforts and clarified how bracket/fairing implementation and measurement environments influence stall onset and recovery.

Tunnel-to-tunnel comparisons of NASA's 5.2%-scale model in the NWB, the 14x22 and the NTF at matched Re_C conditions provided consistent lift and drag trends, but a controlled divergence in pitching moment in the NTF data. These comparisons enable the assessment of tunnel environment and support system influences on pitching moment, which is precisely the kind of facility effect the ecosystem is designed to quantify and feed into CFD calibration and model form assessments, and which is an anchor for CFD sensitivity studies that treat facility differences explicitly rather than as modeling shortcomings.

Testing of the NASA's 2.7%-scale FS model in both the NTF and the ETW provided the opportunity

for another set of tunnel-to-tunnel comparisons at three Re_C. Comparisons between the NASA 5.2%-scale SS and the NASA 2.7%-scale FS in the NTF provided the opportunity to look into semispan vs. full-span installation effects in the wind tunnel. The future planned test of the NASA 2.7%-scale SS, which uses the same port wing as the NASA 2.7%-scale FS model, will provide a greater insight into semispan vs. full-span installation effects in the NTF.

Table 4 – Cross-Campaign Significance for CRM-HL Wind Tunnel Tests

Facility	**Model**	**Configurations Tested**	**Notable Findings**
QinetiQ 5M	10%-scale Semispan	Landing & Takeoff reference setups	Early baseline definition; geometric deviations from final CRM-HL; data used in HLPW4
ONERA F1	5.1%-scale Full-Span	Landing & Takeoff; flap/slat bracket variations	$C_{L_{Max}} \sim 0.16$ higher than NASA semispan; minor geometric deviations (WUSS, sealing)
KHI KLWT	3.23%-scale Full-Span	Landing & Takeoff; modular slat/flap adjustments	CAD alignment confirmed; instrumentation-driven bracket mods
14x22 and NWB	5.2%-scale Semispan	Landing, Takeoff & Cruise; configuration variation and DLR parts	Tunnel-to-tunnel comparison; data reduction and installation variation validation
NASA NTF (T237)	5.2%-scale Semispan	Landing, Takeoff, Iced configurations	High-Reynolds cryogenic runs; tight geometry tolerance verified; continuous vs. pitch pause data collection
NASA NTF (T240)	2.7%-scale Full-Span	Landing: multiple icing scenarios	Systematic repeat runs; cross-scale comparison; semispan vs. full-span comparison
ETW	2.7%-scale Full-Span	Landing; multiple icing scenarios	Systematic repeat runs; tunnel-to-tunnel comparison; continuous vs. pitch pause data collection

3. Data Comparisons

Cross-test comparisons within the CRM-HL ecosystem reveal encouraging consistency in global aerodynamic trends while highlighting facility-specific differences that are critical for CFD validation. At matched lower Reynolds numbers, NASA's 5.2%-scale SS entries in the 14×22 Subsonic Tunnel, NWB, and NTF show close agreement in lift, confirming the repeatability of the ecosystem baseline, the robustness of data-reduction processes in the three tunnels, and confirms that the installation and tunnel differences do not have a large effect on the force and moment data in lift and drag.

NASA's NTF campaigns extend the comparison matrix significantly. The 5.2%-scale SS model in NTF Test 237 spans chord Reynolds numbers from 1.61M to 30M, capturing flight-representative conditions and enabling regression of Reynolds number trends on lift, drag, and pitching moment. The 2.7%-scale FS model in NTF Test 240 and in ETW adds systematic repeat runs and icing configurations, offering controlled studies of Reynolds number effects under full-span geometries and degraded conditions.

Full-span tests introduce additional sensitivities. ONERA's 5.1%-scale full-span campaigns produced a $C_{L_{Max}} \sim 0.16$ higher than NASA's semi-span results at comparable chord Reynolds numbers and a $C_{L_{Max}} \sim 0.11$ higher than NASA's full-span NTF results at comparable chord Reynolds numbers. This difference underscores the influence of bracket and sealing details, wing under-slat surface geometry, and spanwise support effects on stall onset and recovery. KHI's 3.23%-scale full-span dataset provides a valuable mid-scale reference point, aligning closely with the CRM-HL baseline while accommodating instrumentation-driven modifications. Its precise geometry control helps separate genuine aerodynamic differences from hardware allowances. These entries provide direct normalization against ONERA, KHI, and earlier NASA/QinetiQ campaigns, reducing facility bias and improving the robustness of turbulence and transition model assessments near $C_{L_{Max}}$.

Collectively, these comparisons strengthen the foundation for simulation-driven certification. By quantifying Reynolds effects, geometric sensitivities, and facility influences, the CRM-HL dataset enables CFD calibration with unprecedented rigor, reducing predictive uncertainty and accelerating the adoption of advanced modeling techniques.

3.1 Force and Moment Data

A tenet of the CRM-HL model design is modularity, the ability to test the models in multiple ecosystem defined configurations and the ability to test the models with non-original ecosystem components. Over the numerous completed CRM-HL test campaigns many configurations have been tested, Table 5 lists the sub-set of model configurations that are shown in this paper. The ecosystem baseline landing configuration is Landing - Nacelle, with the slat at 30°, the inboard (IB) flap at 40°, the outboard (OB) flap at 37°, the nacelle on, the HTail off and no landing gear (LG), tested at Mach 0.20.

Table 5 – CRM-HL model configurations.

Configuration	Slat	IB Flap	OB Flap	Nacelle	HTail	LG
Landing - Nacelle (L baseline)	30°	40°	37°	on	off	off
Landing - Nacelle & HTail	30°	40°	37°	on	on	off
Landing - HTail	30°	40°	37°	off	on	off
Landing - Clean	30°	40°	37°	off	off	off
Landing/Cruise - HTail	30°	cruise	cruise	off	on	off
Landing/Cruise - Clean	30°	cruise	cruise	off	off	off

The data presented in this paper from the NASA 5.2%-scale SS test in NTF, Test 237, and for the NASA 2.7%-scale FS test in ETW are still considered preliminary data. Final corrections have not been applied, but are expected to be relatively small.

The ONERA 5.1% FS tests in F1 and the NASA 2.7% FS test in ETW utilized continuous data collection, gathering a much higher density of points, at more alphas than the other CRM-HL test campaigns which used pitch pause data collection at discrete alphas. The following data plots show a reduced number of points from what was collected and provided for ONERA 5.1% FS F1 test and NASA 2.7% FS ETW test as a way to keep the plots readable. A set of continuous NTF data is also

shown in one plot specifically comparing continuous to pitch pause data collection, and again, the continuous data was plotted with a reduced number of points for a cleaner plot.

Force and moment balance calibration measurement loads and balance accuracy/uncertainties for the presented test campaigns are shown in Table 6. Model reference dimensions are scaled from the ecosystem full-scale wing reference area, S_{Ref}, of 4130ft^2 (383.7m^2), full-scale semispan S_{Ref} of 2065ft^2 (191.8m^2), full-scale reference chord, C_{Bar}, of 275.8in (7.01m), full-scale reference span, b_{Ref}, of 2323.5in (58.8m), and semispan b_{Ref} of 1156.8in (29.4m). The calibration load and the 2σ or 95% balance uncertainty, $2\sigma BU$, from balance calibrations are presented, along with the calculated force and moment balance accuracies (BA) in engineering units, calculated using Equation 1. The balance accuracies along with the model reference dimensions, scaled to each model, and the tunnel free stream dynamic pressure, Q, can be used to calculate the balance force and moment coefficient accuracies on the data using Equations 2 through 4. Force and moment data are plotted at the model moment reference center (MRC) in the stability axis system, namely lift coefficient, C_L, drag coefficient, C_D, and pitching moment coefficient, C_M but the force and moment coefficient balance accuracies are calculated in the balance axis, which is closely aligned to the model body axis, namely axial force coefficient, C_A, normal force coefficient, C_N, and pitching moment coefficient, C_M, for a consistency through a pitch polar . The stability axis, like the model body axis, is fixed to the aircraft but is rotated with the model's pitch angle, α, to align with the wind direction, shown in Equations 5 and 6, C_M in the stability axis is equal to C_M in the model body axis. A subset of the force and moment plots presented in this paper are shown with error bars for balance accuracy, $\pm 2\sigma BA$, in the model body axis.

$$\text{BalanceAccuracy}_{\text{F\&M}} = BA_{F\&M} = BalanceCalibrationLoad * BA_{2\sigma} \tag{1}$$

$$\text{BalanceAccuracy}_{\text{CA}} = BA_{CA} = \frac{\text{BA}_{\text{AF}}}{Q * S_{Ref}} \tag{2}$$

$$\text{BalanceAccuracy}_{\text{CN}} = BA_{CN} = \frac{\text{BA}_{\text{NF}}}{Q * S_{Ref}} \tag{3}$$

$$\text{BalanceAccuracy}_{\text{CM}} = BA_{CM} = \frac{\text{BA}_{\text{PM}}}{Q * S_{Ref} * C_{Bar}} \tag{4}$$

$$\text{C}_{\text{D}} = \text{C}_{\text{A}} * \cos(\alpha) + \text{C}_{\text{N}} * \sin(\alpha) \tag{5}$$

$$\text{C}_{\text{L}} = \text{C}_{\text{N}} * \cos(\alpha) - \text{C}_{\text{A}} * \sin(\alpha) \tag{6}$$

ONERA's 2σ balance accuracy was quoted to be $\pm 0.001\%$ of the calibration load for all measurements, however ONERA augments that accuracy by a factor of $\sqrt{2}$ [5, Pg.12], the augmented balance accuracy is what is presented in the paper. The balance accuracy for the NASA 2.7%-scale CRM-HL model in the ETW was assumed to have the same balance accuracy as the NASA 2.7%-scale CRM-HL model in the NTF, though the balance was calibrated at ETW for compatibility with the ETW data system.

Table 6 – Force and moment balance measurement loads and accuracy.

Tunnel:	ONERA F1	KHI	14x22	NWB	NTF	NTF & ETW
Model:	5.1%	3.23%	5.2%	5.2%	5.2%	2.7%
S_{REF}	5.43ft^2	4.31ft^2	5.58ft^2	5.58ft^2	5.58ft^2	3.01ft^2
S_{REF}	0.505m^2	0.4m^2	0.519m^2	0.519m^2	0.519m^2	0.28m^2
C_{Bar}	14.14in	8.91in	14.34in	14.34in	14.34in	7.45in
C_{Bar}	0.359m	0.226m	0.364m	0.364m	0.364m	0.189m
Cal Load, AF	±2,203lb	±899.2lb	±500lb	±449.6lb	±1,800lb	±700lb
Cal Load, NF	±11,015lb	±2,248lb	±5,700lb	±1,124lb	±12,000lb	±6,520lb
Cal Load, PM	±312,420$inlb$	±10,620$inlb$	±15,000$inlb$	±21,506$inlb$	±90,000$inlb$	±12,800$inlb$
Cal Load, AF	±9,800N	±4,000N	±2,224.2N	±2,000N	±8,007N	±3,114N
Cal Load, NF	±49,000N	±10,000N	±25,356N	±5,000N	±53,381N	±29,004N
Cal Load, PM	±35,300Nm	±1,200Nm	±1,695Nm	±2,430Nm	±10,169Nm	±1,446Nm
$2\sigma BU_{AF}$	±0.00071%[3]	±0.002%	±0.0019%	±0.003%	±0.0014%	±0.001%
$2\sigma BU_{NF}$	±0.00071%[3]	±0.002%	±0.0007%	±0.003%	±0.0005%	±0.0004%
$2\sigma BU_{PF}$	±0.00071%[3]	±0.002%	±0.0024%	±0.003%	±0.0016%	±0.0005%
BA_{AF}	±1.56lb	±1.8lb	±0.95lb	±1.35lb	±2.52lb	±0.7lb
BA_{NF}	±7.79lb	±4.5lb	±3.99lb	±3.37lb	±6lb	±2.61lb
BA_{PM}	±220.9$inlb$	±21.24$inlb$	±36$inlb$	±64.52$inlb$	±144$inlb$	±6.4$inlb$
BA_{AF}	±6.90N	±8N	±4.23N	±6N	±11.21N	±3.11N
BA_{NF}	±34.60N	±20N	±17.75N	±15N	±26.69N	±11.6N
BA_{PM}	±25.00Nm	±2.4Nm	±4.07Nm	±7.29Nm	±16.27Nm	±0.72Nm

[3] ONERA's balance accuracy is augmented by a factor of $\sqrt{2}$.

3.2 Force and Moment Comparisons

Across facilities and scales, global lift trends are broadly consistent, with key differences near stall at matched Reynolds numbers. At lower Reynolds numbers, $Re_C \sim 1.1M$, NASA's 2.7%-scale FS model and KHI's 3.23%-scale FS model are in close agreement in lift, drag and pitching moment as seen in Figure 9. At $Re_C \sim 1.6M$ NASA's 5.2%-scale SS model shows close agreement in lift and drag across 14×22, NWB, and NTF, as seen in Figure 10, confirming repeatability of the ecosystem baseline and data-reduction methods, however the pitching moment of the NASA 5.2%-scale SS model trends lower in NTF though the error bars are large because of the large pitching moment load range of the balance, and the error bars do fall within range of the 14x22 and NWB C_M data.

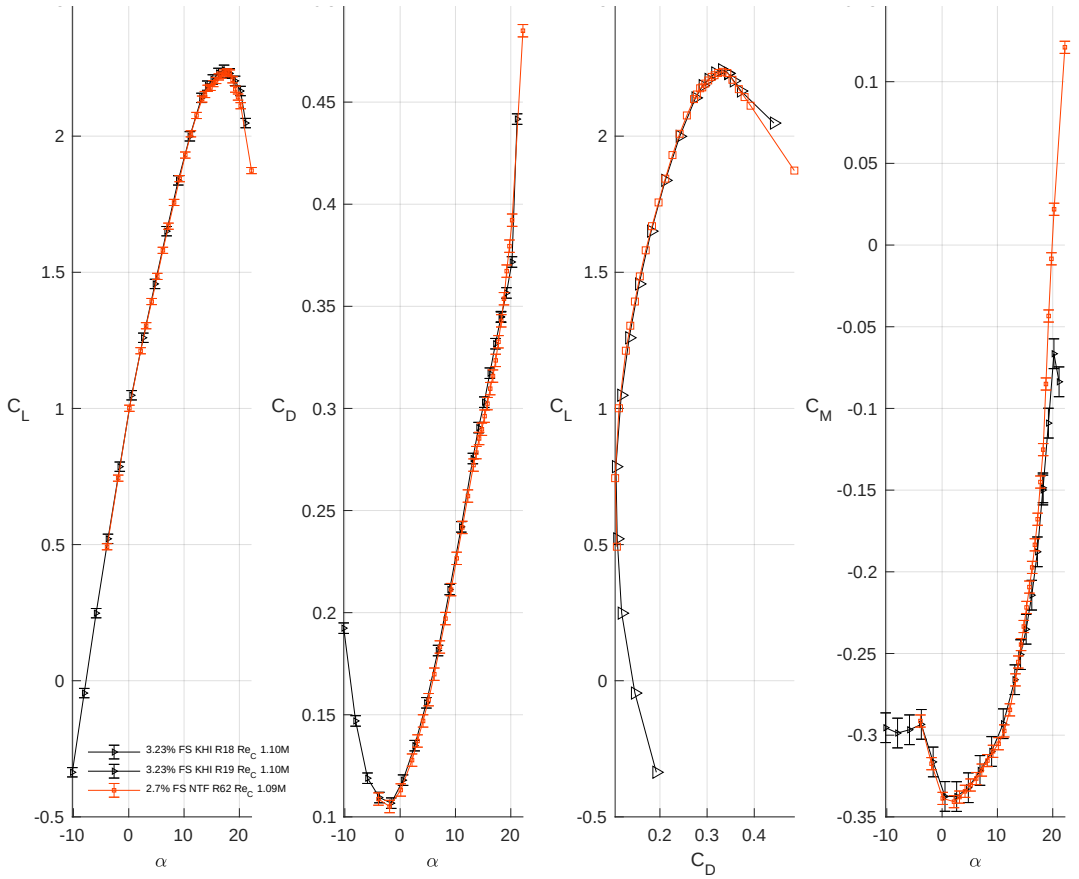


Figure 9 – CRM-HL Landing - Nacelle configuration force and moment $\pm 2\sigma BA$ comparisons at Mach 0.20, Re_C 1.1M.

At matched chord Reynolds numbers, ONERA's 5.1%-scale FS LRM-HL exhibited a $C_{L_{Max}} \sim 0.16$ higher than NASA's semispan model, placing other ecosystem results (e.g., KHI KLWT and later NASA entries) between those bounds, with ONERA having a $C_{L_{Max}} \sim 0.11$ higher than NASA's full-span model at NTF. Figure 11 shows the force and moment comparisons between the ONERA model in F1 and the NASA models in NTF at $Re_C \sim 3.3M - 3.8M$. ONERA and the NASA SS model match well in the linear region of the C_L curve up to $\alpha \sim 10°$ where the NASA SS model begins to trend lower, resulting in a lower $C_{L_{Max}}$. The NASA FS model C_L trends more similarly to the ONERA model, but with a consistently lower C_L magnitude. C_D matches well for the NASA 5.2%-scale SS and the ONERA 5.1%-scale FS at lower angles, below $\alpha \sim 10°$, however around $\alpha \sim 10°$ the drag trend for the two models "bulge" in opposite directions, while the NASA 2.7%-scale FS model drag trends more linear. The ONERA model drag and the NASA 2.7%-scale FS model drag come back together around $\alpha \sim 20°$. NASA's 2.7%-scale FS model C_M trends higher than the other two models.
Figure 12 shows C_L curves for the various CRM-HL models and test campaigns, grouped by configuration (Landing - Nacelle configuration and Landing - Nacelle & HTail configuration) and Re_C, with Figures 13 and 14 showing the same C_L curves zoomed in on the linear regions and the $C_{L_{Max}}$ regions of the C_L curves, respectively. The first three C_L vs. α plots in the three figures are for the models

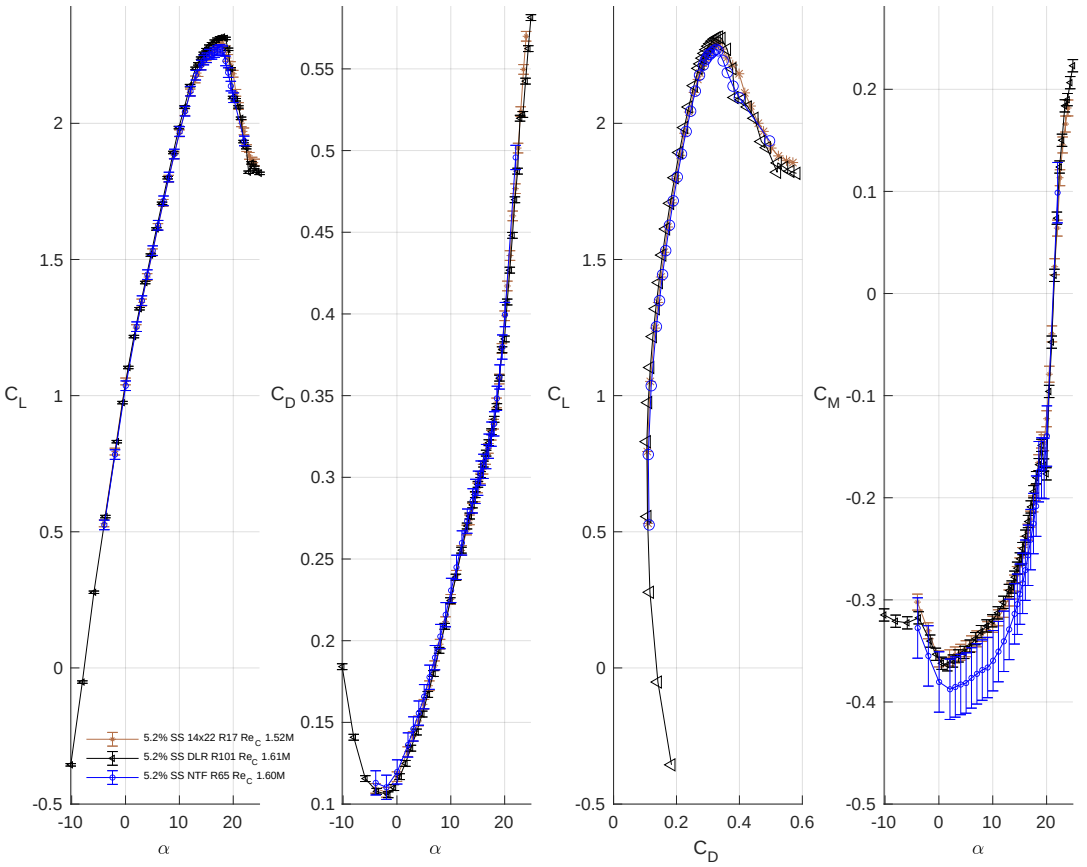


Figure 10 – Tunnel-to-tunnel force and moment $\pm 2\sigma BA$ comparisons of the NASA 5.2%-scale semispan model in the Landing - Nacelle configuration at Mach 0.20, Re_C 1.6M

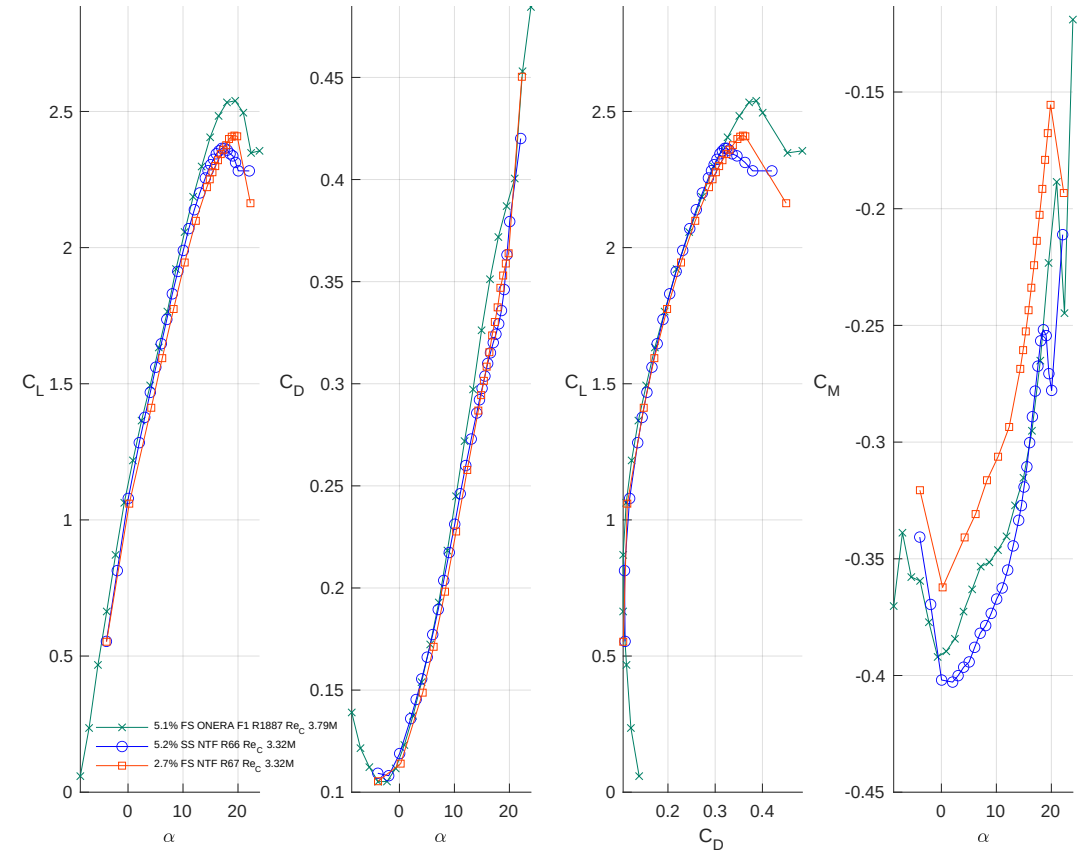


Figure 11 – CRM-HL Landing - Nacelle configuration force and moment comparisons at Mach 0.20, Re_C 3.3M and 3.8M.

in the Landing - Nacelle configuration, and the 4th plot is with the models in the Landing - Nacelle & HTail configuration. The C_L curves for all the CRM-HL tests have similar trends, with a slight variation in the linear region for the NASA semispan model which begins losing lift and not staying linear around $\alpha \sim 8°$, staying close to the ONERA F1 C_L data until $\alpha \sim 16°$ at Re_C 1.6M and $\alpha \sim 11°$ at Re_C 5.9M, resulting in a lower $C_{L_{Max}}$ occurring at a lower α than the other CRM-HL models across all tunnels. The lower $C_{L_{Max}}$ on the NASA 5.2%-scale model is likely a semispan mounting effect that will be investigated with the future testing of the NASA 2.7%-scale model in the semispan configuration in the NTF. The magnitude of C_L for the NASA full-span model in NTF consistently trends lower in the linear region of the C_L curves at Re_C above 1.1M, though the same model at ETW trends much more closely with the other curves. The ONERA model in F1 consistently has a higher $C_{L_{Max}}$, and it does not begin losing lift until a higher alpha, though $C_{L_{Max}}$ does occur at similar alphas for the ONERA model and the NASA full-span model. Also worth noting is that the ONERA F1 data and the ETW data have a much higher density of alpha data because of the continuous pitch data versus point pause data at discrete alphas in other test campaigns, so pinpointing the α at which $C_{L_{Max}}$ occurs is more accurate.

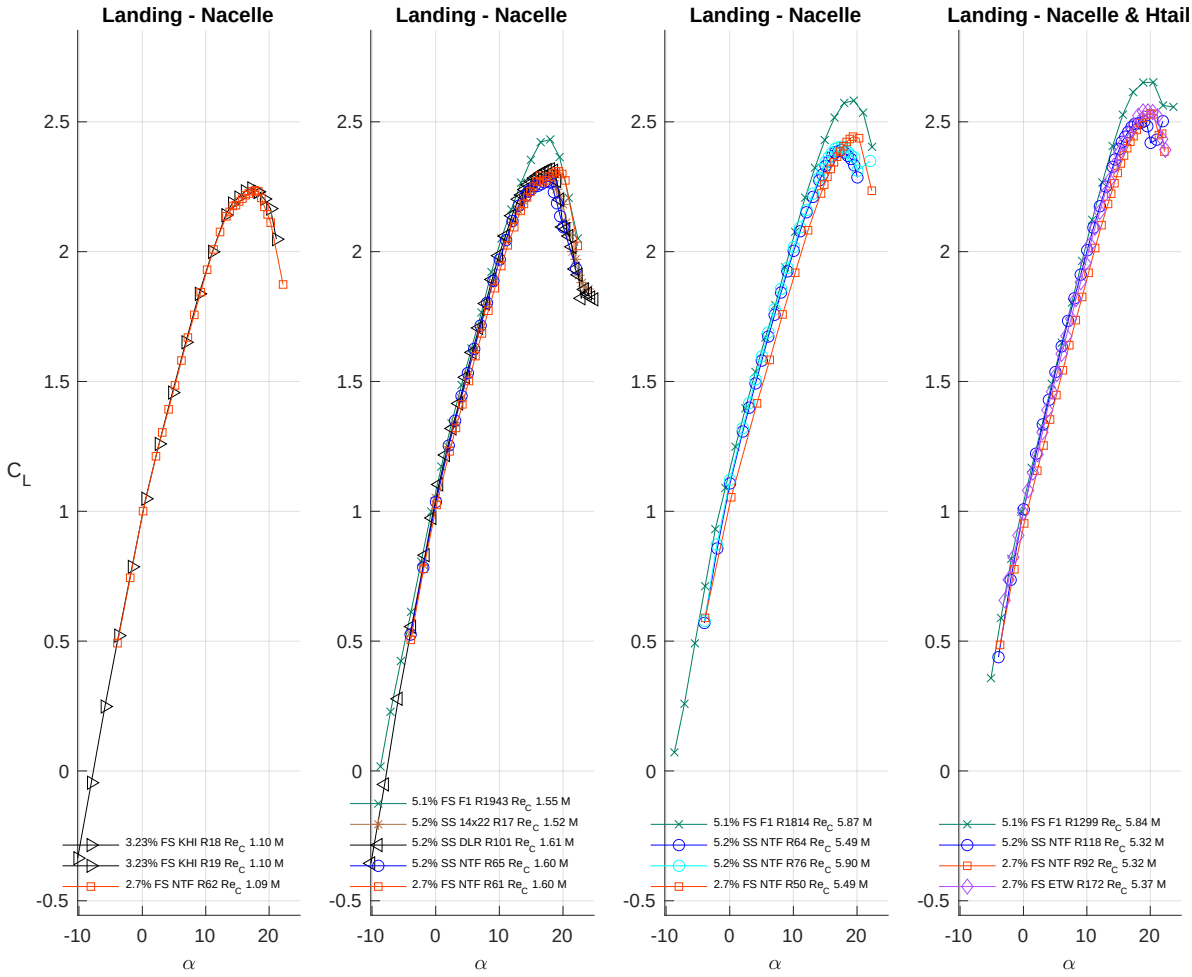


Figure 12 – C_L vs. α CRM-HL Landing - Nacelle configuration and Landing - Nacelle & HTail configuration test and model comparisons at Mach 0.20 at varying Re_C.

The 2.7%-scale FS NTF Test 240 and ETW test further extends the $C_L/C_{L_{Max}}$ matrix via the air-only (NTF mid-2025) and cryogenic (ETW early-2026, NTF planned for early 2027) testing phases at Mach 0.20 and angles of attack from $-4°$ to $22°$, adding systematic repeat runs and comparison points across ecosystem campaigns. Figure 15 shows force and moment comparisons and Figure 16 shows C_L vs. alpha curves at various Re_C of the NASA 2.7%-scale CRM-HL model in the Landing - Nacelle & HTail configuration in the NTF and in ETW at Mach 0.20. At the lowest comparison Re_C of 1.1M the model repeats well between the two tunnels, however as Re_C increases the ETW data

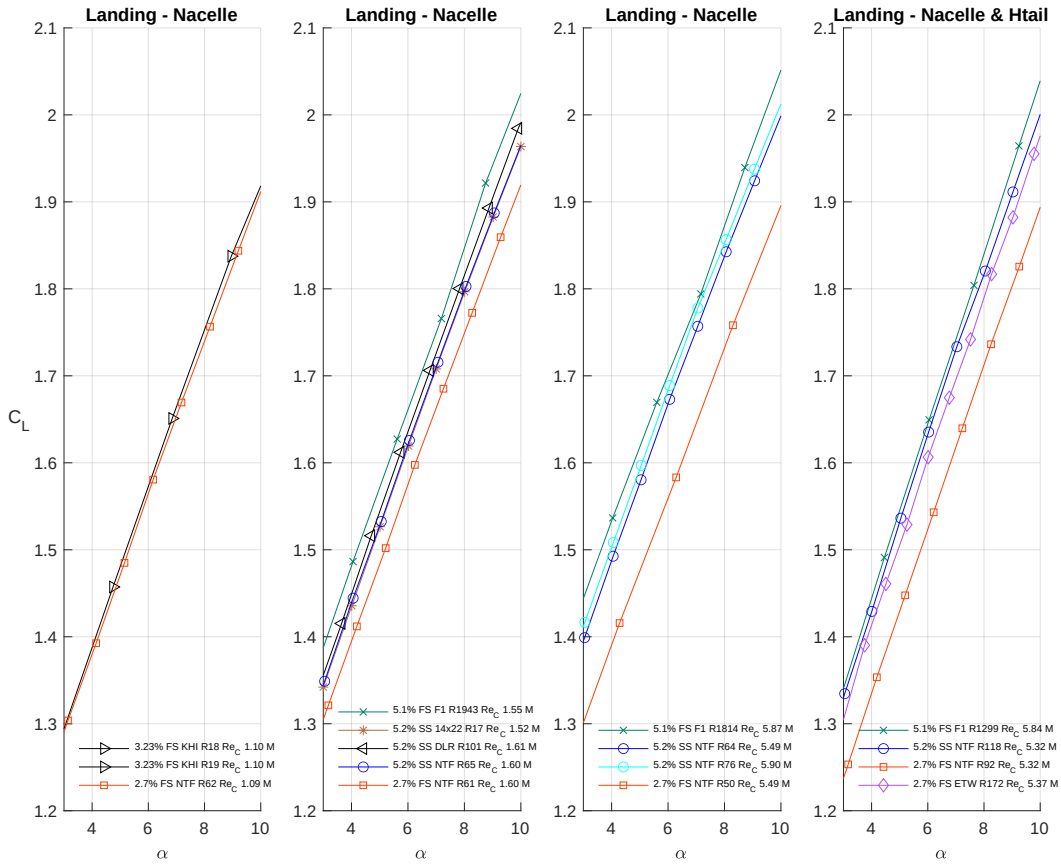


Figure 13 – C_L vs. α CRM-HL Landing - Nacelle configuration and Landing - Nacelle & HTail configuration test and model comparisons at Mach 0.20 at varying Re_C, linear region zoom.

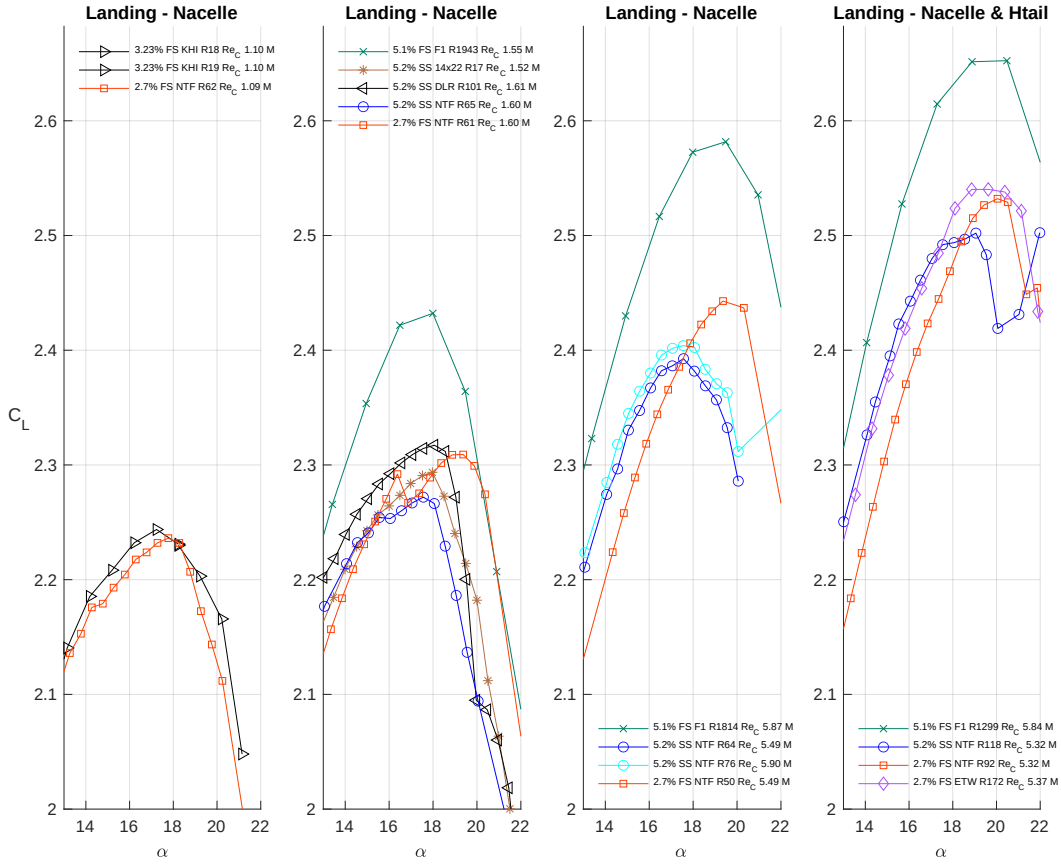


Figure 14 – C_L vs. α CRM-HL Landing - Nacelle configuration and Landing - Nacelle & HTail configuration test and model comparisons at Mach 0.20 at varying Re_C, $C_{L_{Max}}$ zoom.

magnitude increases more than the NTF C_L magnitude. Post-test inspections of the NASA 2.7%-scale FS model at the NTF it was discovered that the strakes, at the wing to fuselage junction, were undercut slightly. The undercut was filled in for the ETW data shown in this paper. Of note is that a very small amount of the ETW increase in C_L is from the strake fix on the model between the two tests. At the three Re_C comparisons run between NTF and ETW the drag falls on top of each other, however C_M at NTF is slightly higher in magnitude for all Reynolds numbers. The magnitude differences in C_L and C_M for the NASA 2.7%-scale CRM-HL model in NTF and ETW are being investigated.

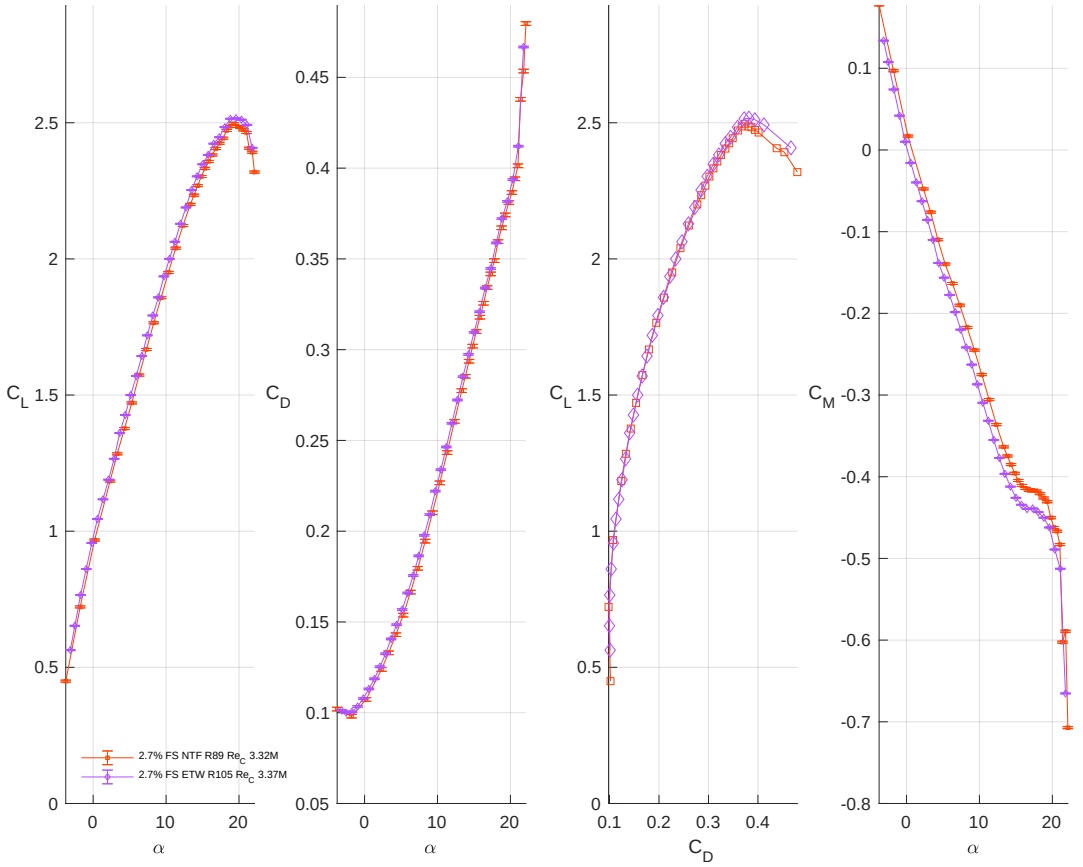


Figure 15 – Tunnel-to-tunnel force and moment $\pm 2\sigma BA$ comparisons of the NASA 2.7%-scale full-span CRM-HL model in the Landing - Nacelle & Tail configuration, Mach 0.20, $Re_C \sim 3.33M$.

Observed differences between facilities and model implementations should be studied within the context of high-lift flow physics. Variations in lift, drag, and pitching moment can result from differences in transition location, local separation onset, wake development, and multi-element interactions between the slat, main element, and flap system. As stall is approached, relatively small changes in boundary-layer state or local geometry can alter separation progression, resulting in measurable changes in $C_{L_{Max}}$, drag growth, and pitching moment characteristics. Consequently, cross-test comparisons provide insight not only into facility-to-facility agreement but also into the underlying aerodynamic sensitivities that drive high-lift performance.

3.3 Drag Coefficient

The drag comparisons between KHI and the NASA 2.7%-scale SS model, Figure 9, for the NASA 5.2%-scale SS model between 14×22, NWB, and NTF, Figure 10, and for the NASA 2.7%-scale FS model between NTF and ETW, Figure 15, show good agreement. The higher Reynolds number range at NTF, due to cryogenic operation, Mach 0.20–0.35, Re_c 1.61M–30M, reveals reduced viscous contributions and shifts in separation onset consistent with certification-level physics, framing the reference for LES/WMLES validation. ONERA's pressurized F1 data contribute low-speed drag characteristics under elevated test-section pressures, offering a complementary tunnel environment to probe sensitivity to bracket/sealing and WUSS geometry while maintaining tight geometric tolerances verified by

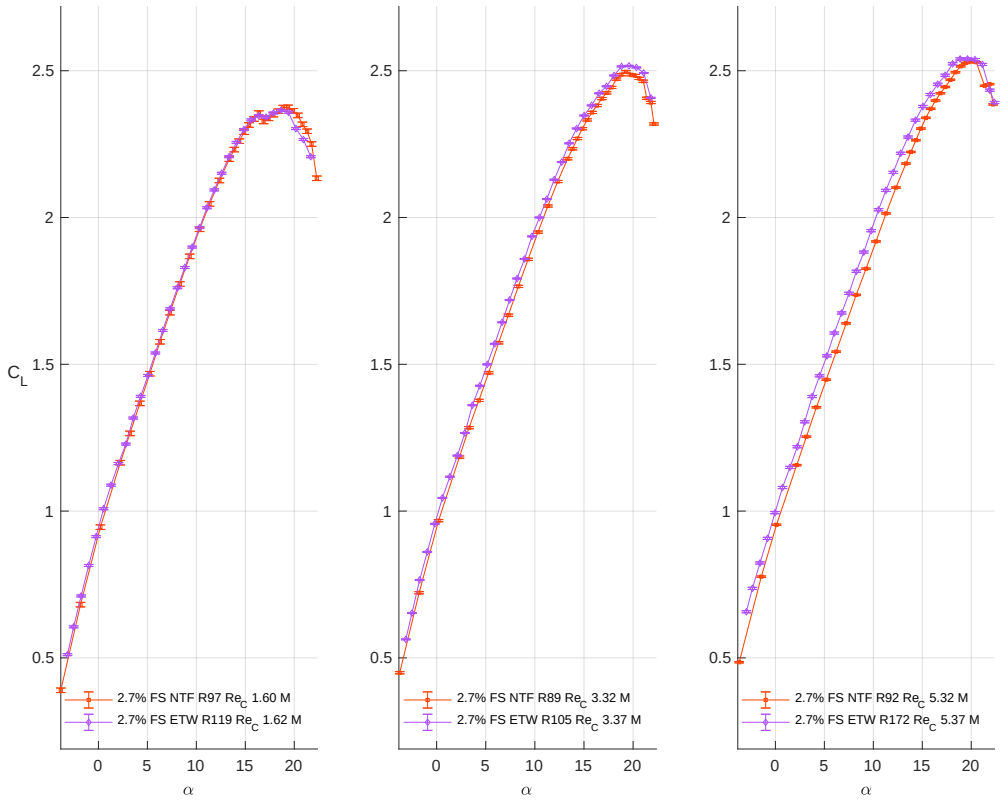


Figure 16 – Tunnel-to-tunnel C_L $\pm BA_{CN}$ vs. α comparisons of the NASA 2.7%-scale full-span CRM-HL model in the Landing - Nacelle & Tail configuration, Mach 0.20 at varying Re_C.

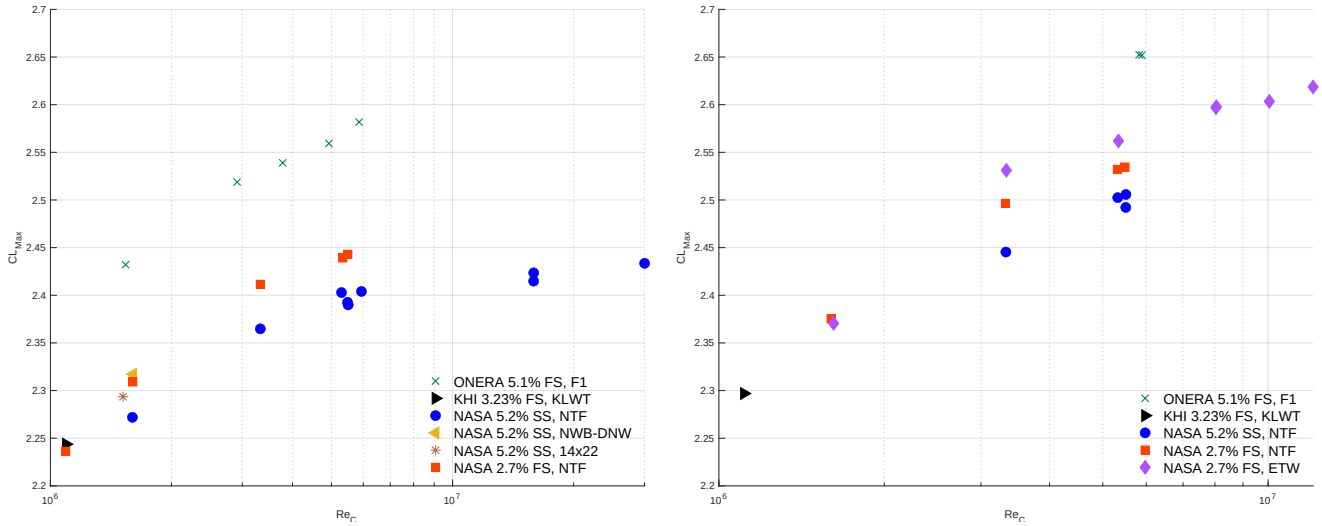
inspection.

3.4 Pitching Moment

A notable outcome is the pitching-moment divergence observed for the 5.2%-scale SS between NTF and the 14×22/NWB tests at matched low Reynolds number—despite strong agreement in lift and drag seen in Figure 10 and for the 2.7%-scale FS between NTF and ETW seen in Figure 15 . Given the confirmed repeatability and independent balances and data reductions, this CM difference is treated as a known and quantifiable difference between test installations that can be used for CFD sensitivity studies, providing the opportunity to study the influences of support system, tunnel environment, and flow quality. These controlled variations provide essential data for turbulence and transition model calibration, ensuring that discrepancies are understood and accounted for rather than attributed to modeling limitations alone.

3.5 Reynolds Number Effects

The influence of Reynolds number on aerodynamic performance is one of the most critical findings from CRM-HL campaigns. NASA's NTF Test of the 5.2%-scale SS model spans chord Reynolds numbers from 1.61M to 30M, enabling systematic regression of Reynolds trends on lift, drag, and pitching moment. These data confirm that increasing Reynolds number increases lift and delays flow separation, shifting stall onset, valuable information for improving $C_{L_{Max}}$ predictions in CFD. The 2.7%-scale FS model NTF Test 240 and ETW test extends this envelope through air-phase and cryogenic entries, providing controlled comparisons under full-span geometries and icing conditions. Together, these campaigns supply benchmark-quality data for calibrating turbulence and transition models, ensuring CFD predictions remain robust across the full Reynolds spectrum relevant to certification.
Figure 17 shows $C_{L_{Max}}$ Reynolds number trends for the test campaigns, for both the Landing configuration with and without the horizontal tail installed. All test campaigns followed the expected Reynolds number trends within test. Table 7 lists the recorded $C_{L_{Max}}$ and the α where $C_{L_{Max}}$ occurred for all data runs plotted in this paper, separated by model configuration, in order of Re_C of the runs. Again note that the NASA 5.2% SS NTF data and the NASA 2.7% FS ETW are considered preliminary.



(a) Landing - Nacelle.

(b) Landing - Nacelle & HTail.

Figure 17 – $C_{L_{Max}}$ at Re_C for CRM-HL test campaigns, Mach 0.20.

Increasing Reynolds number affects high-lift performance through several coupled physical mechanisms. As Reynolds number increases, the boundary layer becomes thinner relative to the local geometry and gains greater resistance to adverse pressure gradients. This delays the onset of flow separation on the wing, slat, and flap elements, allowing the high-lift system to maintain attached flow to higher angles of attack allowing for higher $C_{L_{Max}}$ value. Additionally, the resulting increase in circulation improves lift generation throughout the linear portion of the lift curve. For multi-element high-lift configurations such as the CRM-HL, Reynolds number also affects the interaction between slat wakes, flap loading, and boundary-layer transition. At lower Reynolds numbers, thicker boundary layers and earlier separation can alter pressure recovery on the more downstream elements, leading to earlier degradation of lift performance. These effects become particularly important near $C_{L_{Max}}$, where small changes in separation location or progression can produce significant changes in maximum lift and stall characteristics.

Table 7 – $C_{L_{Max}}$ run list.

Config	Test	Run	Mach	Re_C^6	Q (psf)	Q (kPa)	α_{Max}	$\pm BA_{CN}$	$C_{L_{Max}}$
LDG - Nac	NASA 2.7% FS, NTF	62	0.2	1.09	77	3.70	17.8°	.0113	2.24
	KHI 3.23% FS, KLWT	18	0.2	1.1	61	2.90	17.2°	.0172	2.24
	NASA 5.2% SS, 14x22	17	0.2	1.52	57	2.70	18.0°	.0124	2.29
	ONERA 5.1% FS, F1[3]	1943	0.2	1.55	57	6.20	18.0°	.0111	2.43
	NASA 5.2% SS, NTF[2]	65	0.2	1.6	61	2.90	17.6°	.0176	2.27
	NASA 2.7% FS, NTF	61	0.2	1.6	112	5.40	19.4°	.0077	2.31
	NASA 5.2% SS, NWB	101	0.2	1.61	59	6.50	18.1°	.0045	2.32
	ONERA 5.1% FS, F1[3]	1901	0.2	2.92	108	11.90	19.5°	.0058	2.52
	NASA 5.2% SS, NTF[2]	69	0.2	3.31	133	6.40	17.7°	.0081	2.37
	NASA 5.2% SS, NTF[2]	66	0.2	3.32	133	6.40	17.6°	.0081	2.36
	NASA 2.7% FS, NTF	67	0.2	3.32	234	11.20	19.3°	.0037	2.41
	ONERA 5.1% FS, F1[3]	1887	0.2	3.79	139	15.20	19.5°	.0045	2.54
	ONERA 5.1% FS, F1[3]	1871	0.2	4.93	182	19.90	19.7°	.0035	2.56
	NASA 5.2% SS, NTF[2]	78	0.2	5.32	134	6.40	17.6°	.0081	2.40
	NASA 2.7% FS, NTF	51	0.2	5.34	370	17.70	19.3°	.0023	2.44
	NASA 5.2% SS, NTF[2]	82	0.2	5.49	138	6.60	17.0°	.0078	2.39
	NASA 5.2% SS, NTF[2]	64	0.2	5.49	207	9.90	17.6°	.0052	2.39
	NASA 2.7% FS, NTF	50	0.2	5.49	381	18.20	19.4°	.0023	2.44
	ONERA 5.1% FS, F1[3]	1814	0.2	5.87	217	23.80	19.5°	.0029	2.58
	NASA 5.2% SS, NTF[2]	76	0.2	5.9	149	7.10	17.6°	.0072	2.40
	NASA 5.2% SS, NTF[2]	94	0.2	15.9	239	11.40	17.6°	.0045	2.42
	NASA 5.2% SS, NTF[2]	98	0.2	15.91	157	7.50	17.6°	.0068	2.41
	NASA 5.2% SS, NTF[2]	96	0.2	30.04	294	14.10	17.6°	.0036	2.43
LDG - Nac & HT	KHI 3.23% FS, KLWT	9	0.2	1.11	62	3.00	17.2°	.0170	2.30
	NASA 2.7% FS, NTF	97	0.2	1.6	112	5.40	19.4°	.0077	2.38
	NASA 2.7% FS, ETW [2]	119	0.2	1.62	114	12.50	18.9°	.0033	2.37
	NASA 2.7% FS, NTF	94	0.2	3.32	233	11.20	19.3°	.0037	2.49
	NASA 2.7% FS, NTF	89	0.2	3.32	234	11.20	19.3°	.0037	2.50
	NASA 5.2% SS, NTF[2]	46	0.2	3.33	133	6.40	19.1°	.0081	2.45
	NASA 2.7% FS, ETW [2]	105	0.2	3.37	236	25.90	20.8°	.0016	2.53
	NASA 5.2% SS, NTF[2]	118	0.2	5.32	134	6.40	22.0°	.0080	2.50
	NASA 2.7% FS, NTF	92	0.2	5.32	369	17.70	20.0°	.0024	2.53
	NASA 2.7% FS, ETW [2]	172	0.2	5.37	103	11.30	20.6°	.0037	2.56
	NASA 5.2% SS, NTF[2]	117	0.2	5.49	138	6.60	19.1°	.0078	2.51
	NASA 2.7% FS, NTF	90	0.2	5.49	381	18.20	20.0°	.0023	2.53
	NASA 5.2% SS, NTF[2]	47	0.2	5.5	207	9.90	22.1°	.0052	2.49
	ONERA 5.1% FS, F1[3]	1299	0.2	5.84	212	23.30	20.5°	.0030	2.65
	ONERA 5.1% FS, F1[3]	1788	0.2	5.87	217	23.90	19.3°	.0029	2.65
	ONERA 5.1% FS, F1[3]	1789	0.2	5.92	218	23.90	19.1°	.0029	2.65
	NASA 2.7% FS, ETW [2]	166	0.2	8.07	155	17.00	20.5°	.0025	2.60
	NASA 2.7% FS, ETW [2]	192	0.2	8.08	231	25.30	20.4°	.0016	2.60
	NASA 2.7% FS, ETW [2]	158	0.2	10.1	194	21.30	20.6°	.0020	2.60
	NASA 2.7% FS, ETW [2]	137	0.2	12.11	233	25.60	20.6°	.0016	2.62
LDG - Htail	ONERA 5.1% FS, F1[3]	1533	0.2	5.85	206	22.60	20.5°	.0030	2.68
LDG - Clean	NASA 5.2% SS, 14x22	19	0.2	1.5	57	2.70	18.0°	.0125	2.29
	NASA 5.2% SS, NTF[2]	53	0.2	5.47	207	9.90	19.1°	.0052	2.36
LDG/C - Clean	NASA 5.2% SS, 14x22	21	0.2	1.58	57	2.70	21.5°	.0125	1.69
LDG/C - Htail	ONERA 5.1% FS, F1[3]	1619	0.2	5.83	211	23.10	23.3°	.0030	2.07

[2] NASA 5.2%-scale SS NTF Test 237 data and NASA 2.7%-scale FS in ETW data are PRELIMINARY.
[3] ONERA's balance accuracy is augmented by a factor of $\sqrt{2}$.

4. C_L Delta Considerations and Investigations

After the ONERA and NASA test comparisons showed the ~ 0.16 $C_{L_{Max}}$ difference in the data, a thorough investigation into the cause was started. The factors affecting aerodynamic values when testing in wind tunnels that have been, and are being considered and investigated are shown in Table 8.

Table 8 – Wind tunnel testing factors affecting C_L

Model OML	**Model-to-Tunnel Installation**	**Tunnel Flow**	**Data Reduction**
SS vs. FS	Fouling	Non-uniform flow	Corrections applied
Aeroelastic deformation	Bridging the balance	Wall effects	Model constants
Trip dot location & effectiveness	SS Flow inside of the fuselage cavity	Wall boundary layer	
Model leak paths		Tunnel flow conditions (Mach, temperature, pressure)	
		Continuous vs. Point pause operation	

4.1 Model OML Considerations and Investigations

Each model in the CRM-HL ecosystem of models has some slight OML variations from the ecosystem geometry, some OML variations are by design to fit instrumentation or for manufacturing purposes, and some OML variations are from the manufacturing of the individual models resulting in the as-built model OML not matching the as-designed OML. When manufacturing a wind tunnel model, trade-offs are always made between accuracy of the model, time to manufacture the model and final cost of the model. Models are specified to be built to within a certain tolerance of the as-designed OML and quality assurance checks are done on the final as-built model to either find areas outside of the designated tolerance that need to be corrected, or recorded for reference.

As noted previously, ONERA's final design was completed before the ecosystem baseline definition was fully standardized, resulting in some minor OML deviations from the final CRM-HL baseline OML, notably some slight IB slat positioning and trim differences, the IB flap to fuselage sealing is slightly deeper on the ONERA model than in the ecosystem baseline definition, and the ONERA outboard WUSS has the old geometry definition and positioning which differs by 0.024 inches (0.6 mm) at the outboard section relative to the CRM-HL baseline geometry. An extensive geometric inspection of the as-built ONERA 5.1%-scale LRM-HL wing, done using a Faro Quantum system[4] across 15 wing sections [5, Pg.4 Table2] confirmed the model accurately conforms to the design. The inspection confirmed high accuracy placement precision for slats and flaps, which is critical to gap definition and repeatability, as noted by Mouton et al. [5], and the maximum positioning error of slats and flaps was within 0.13% of the wing mean aerodynamic chord, demonstrating exceptional build precision.

The OML of the KHI 3.23%-scale CRM-HL model was designed from the ecosystem reference configuration defined in Lacy and Clark [2] using the Reference Geometry CAD files on the Common Research Model webpage [18]. The flap track fairings and the slat tracks were designed from the NASA 5.2%-scale definition, which had to be grown relative to the wing and re-designed slightly to accommodate the pressure tubing running from the flaps to the wing. In accordance with the ecosystem recommendations the flap track and slat track variations from baseline ecosystem design were in height and not width. The final CAD model for the as-designed KHI CRM-HL was compared to the HLPW5 workshop CAD model, with "no difference found between the two CAD models" [7].

The NASA 5.2%-scale CRM-HL model slat brackets and flap track fairings were grown from the ecosystem standard in order to house pressure tubing running from the slats and flaps to the main

[4]No Federal Government endorsement is intended or implied.

wing spar instrumentation trough. In accordance with the ecosystem recommendations, the slat brackets and the flap track fairing variations from baseline were in height and not width. The tolerances prescribed to the model manufacturer for the NASA 5.2%-scale model were specified to be $\pm$ 0.003in (0.075mm, full-scale 0.58in, 14.42mm) surface contour, $\pm$ 0.0015in (0.038mm, full-scale 0.29in, 7.31mm) slat surface contour, and $\pm$ 0.01in (0.254mm, full-scale 1.92in, 48.85mm) planform tolerance. An EDGE FaroArm[4] measurement system was used to inspect hundreds of points on the full wing assembly in all configurations by the model manufacturer. The inspection of the as-built model was compared to the as-designed NASA 5.2%-scale CRM-HL model CAD, and showed the model to be very accurate, with only a few areas of the wing slightly outside of prescribed manufacturing tolerances compared to the as-designed CAD. Because the balance used in the NWB was unable to handle the weight of the complete NASA 5.2%-scale model, DLR built their own composite fuselage to hold the NASA 5.2%-scale port wing. The DLR fuselage had the same OML and labyrinth seal as the NASA fuselage.

The NASA 2.7%-scale FS model was designed using the CAD geometry with the 0.2 inch (5.08mm) full-scale lofted trailing edges because the trailing edges would have been too thin otherwise for the scale of the model. The slat brackets and flap track fairings were also grown from the ecosystem standard in height, not width, to accommodate pressure tubing. The NASA 2.7%-scale FS model OML was inspected by the model designer in the fully built up configuration using a Faro arm[4], with only minor deviations outside of the design tolerances listed in Ertsgaard et. al. [19]. A more thorough scan of the model is planned to be done at in the near future.

Another check on the model OML affecting the C_L magnitude difference was looking at nacelle, flap and horizontal tail effects. Figure 18 show configuration variation comparisons between the ONERA 5.1%-scale FS LRM-HL model and the NASA 5.2%-scale SS CRM-HL model, nacelle on versus nacelle off, landing flaps (IB flap = 40°, OB flap = 37°) versus cruise/stored flaps, and horizontal tail on versus horizontal tail off. It can be seen that the C_L magnitude differences remain with the changing of model parts, and the configuration effects of the models are comparable, giving confidence that the nacelle, the flaps, and the horizontal tail are not responsible for the difference in C_L and that the OML on these parts are comparable.

From the above quality assurance analysis and CAD analysis, the team considers each of the CRM-HL ecosystem models to be an accurate representation of the CRM-HL ecosystem geometry, though it is important to understand the geometry difference between models.

Historically some differences in aerodynamic values have been seen between semispan and full-span models. For some configurations with similar lift levels to CRM-HL the difference is about ΔC_L = 0.02 - 0.03, which could account for the differences seen in the NASA 5.2%-scale SS CRM-HL model and the NASA 2.7%-scale FS CRM-HL model in NTF, and about 1/3 of the ΔC_L observed between the NASA 5.2%-scale SS and ONERA data. **The differences in the linear region of the C_L lift curve slopes and the lower $C_{L_{Max}}$ between the NTF tests of the NASA 5.2%-scale SS and the NASA 2.7%-scale FS (Figure 19) warrant further investigation into semispan testing effects on forces and moments.** Testing of the NASA 2.7%-scale model in the semispan configuration, using the port wing from the full-span model, planned for testing in the NTF in late 2027 will help answer semispan versus full-span model effect questions.

The CRM-HL baseline OML was designed to match the OML of an airplane in loading from flight, not while it is sitting on the ground. While wind tunnel models are relatively stiff they do still bend and twist slightly while under load during testing. This deformation of the wing changes the wing OML which changes how the wing is loaded. If the model wing were to bend or twist "too much" it would affect the lift on the model, along with the other forces and moments. Wing bending and wing twist were recorded using model deformation targets in the NTF test [21] and the ETW test.

The maximum wing bending measured on the NASA 5.2%-scale NTF test [10] was 1.16 inches (29.5mm), 0.08 normalized by chord (14.3in) at the tip of the wing, and the max twist was 1.07°, both at Mach 0.2, Re_C 30M, dynamic pressure (Q) 295psf (14.1kPa) at alphas 18.5°, and 16°, respectively. The maximum wing bending measured on the NASA 2.7%-scale NTF (air-only) test was 0.67 inches

[4]No Federal Government endorsement is intended or implied.

[4]No Federal Government endorsement is intended or implied.

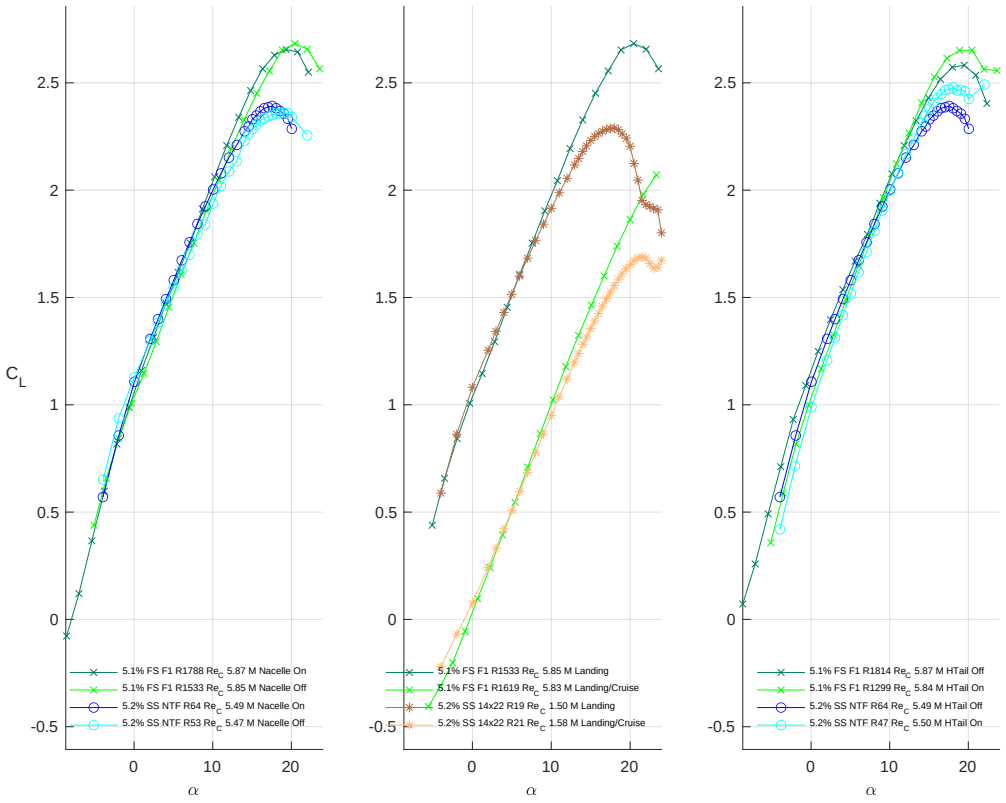


Figure 18 – C_L vs. α, landing configuration variation comparisons, Mach 0.20.

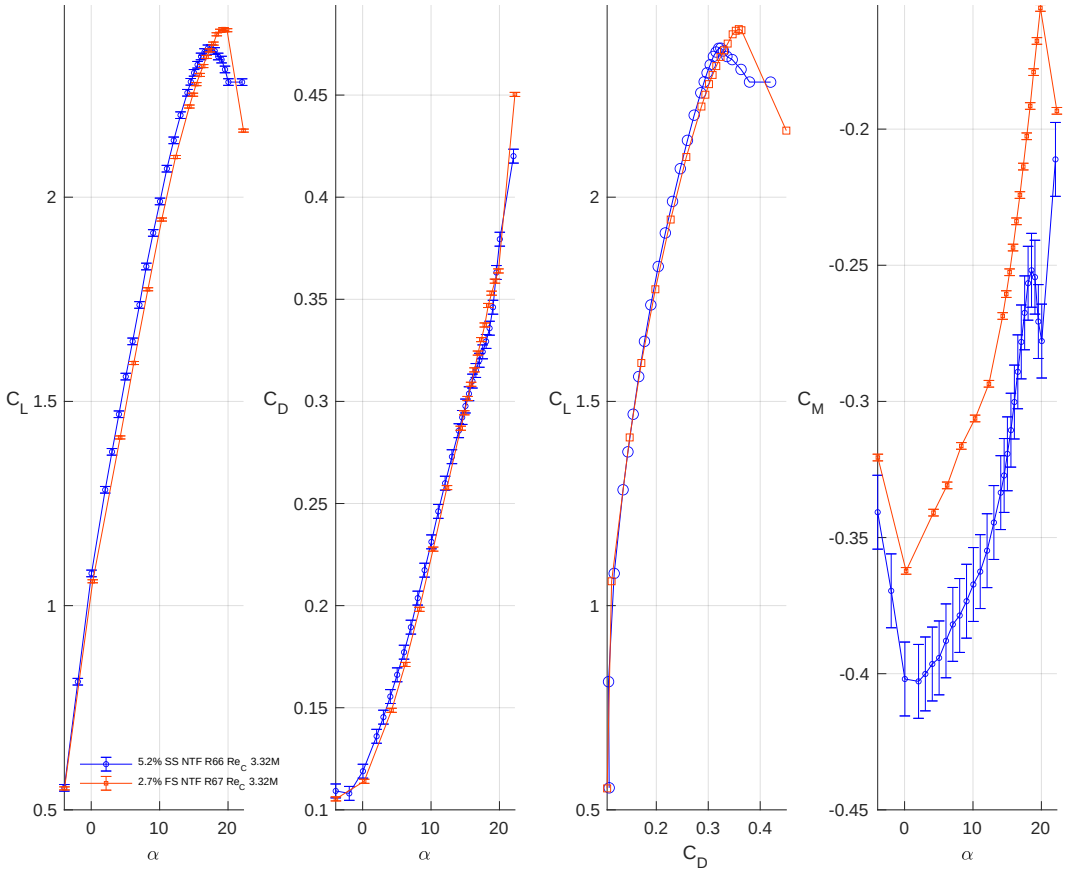


Figure 19 – Force and moment $\pm 2\sigma BA$ comparisons of the NASA 5.2%-scale SS model and the NASA 2.7%-scale FS model in the Landing - Nacelle configuration in NTF at Mach 0.20, Re_C 3.32M.

(17mm), 0.09 normalized by chord (7.4in) at the tip of the wing, at Mach 0.2, Re_C 5.33M, Q 370psf (17.7kPa), and alpha 19.8°, and the maximum measured twist was 0.86 deg, at Mach 0.2, Re_C 5.49M, Q 381psf (18.2kPa) alpha 17.8°. The maximum wing bending measured on the NASA 2.7%-scale ETW test was 1.42 inches (22.3mm), 0.12 normalized by chord, and the maximum measured twist was 1.43°, both at Mach 0.2, Re_C 16M, Q 393psf (18.8kPa) alpha 19° **The amount of wing bending and twist on the NASA 5.2%-scale SS CRM-HL model and on the NASA 2.7%-scale FS CRM-HL model were as expected, and likely did not cause a large reduction in lift from the design, however a deeper look in to the effects of wing deformation on the measured forces is planned for the future using CFD.**

Trip dots are used on wind tunnel models to force transition of the flow from laminar to turbulent in order to match anticipated flight conditions and to more closely match what CFD models. The CRM-HL ecosystem has defined a standard trip dot application scheme for location of transition strips, however since each tunnel has unique capabilities, and each model was built to a different scale, it is up to the ecosystem partners to determine the best transition height to use for their testing. Transition height is generally selected based on an estimated boundary layer height on the model based on tunnel pressure, Mach, and temperature condition, and also based on the X distance back from a stagnation point location placement.

All tests used trip dots for transition, at varying heights but with a common diameter of 0.05 inches (1.27 mm) and a common center-to-center spacing of 0.10in (2.54mm). The ONERA 5.1%-scale FS F1 test used trip dot heights of 0.0045in (0.11mm) and 0.005in (0.13mm), the KHI 3.23%-scale KLWT test and the NASA 5.2%-scale SS 14x22 test used a trip dot height of .0114in (0.29mm), the NASA 5.2%-scale SS in NWB and NTF used a trip dot height of 0.005in (0.13mm), and the NASA 2.7%-scale FS tests in NTF and ETW used a trip dot height of 0.0031in (0.01mm). The NASA Q5m 10%-scale, the KLWT 3.23%-scale, the NASA 5.2%-scale, and the NASA 2.7%-scale tests all followed the ecosystem defined trip dot scheme, scaling down the full scale definition. For high Reynolds number testing in the NTF and ETW trip dots were removed from the wings. The ONERA test was run using a different trip dot scheme from the full-scale baseline defined scheme. Table 9 lays out the ecosystem defined trip dot scheme in full=scale, the trip dot scheme used on each model, and the difference from the ecosystem baseline trip dot scheme to the ONERA trip dot scheme (Δ Baseline). The NASA models used the ecosystem prescribed transition scheme, but no study was done to confirm flow transition at the location of the trip dots. **A trip dot study is planned during the NTF high Re test of the NASA 2.7% CRM-HL FS model planned for spring of 2027.**

A consideration for the lower lift on the NASA 5.2%-scale CRM-HL model was a potential leak path from the lower surface of the wing to the upper surface of the wing. The underside of the NASA 5.2%-scale CRM-HL was heavily taped during the DLR and 14x22 test entries, but it was still decided to do a full leak path study during the NTF test entry to be sure that no potential leak paths were missed. During the NTF test a set of 5 runs were done, each with an increasing amount of tape on the wing, both on the lower and upper surface. Areas of the wing that were carefully taped or filled included cover plates, the flow visualization D-shaped insert, the spoiler to spar seam, the strake to wing seam at the leading edge, the WUSS insert, the wing to fuselage junction, and the flap to fuselage junction. For the final taping run all seams were taped over. The wing taped runs were plotted against the clean wing. No increase in lift was seen with the wing taped on all seams vs. the clean wing [10] **confirming that there are no significant leak paths on the NASA 5.2%-scale CRM-HL wing.**

The consistently higher $C_{L_{Max}}$ observed in the ONERA F1 data relative to both NASA semispan and full-span datasets likely reflects a combination of Reynolds-number-dependent flow physics and localized geometric implementation differences. High-lift configurations are particularly sensitive to transition location, boundary-layer development, and separation progression near stall. Small differences in WUSS geometry, slat and flap bracket implementation, gap sealing strategies, and local surface contouring can influence pressure recovery and modify the development of three-dimensional separation structures.These differences are amplified near $C_{L_{Max}}$ because stall progression in multi-element systems is often governed by localized flow breakdown that subsequently propagates spanwise. As a result, relatively minor geometric differences may have little impact in the linear lift region while producing measurable differences in maximum lift and stall onset. The hope is to quantify these

Table 9 – Trip dot locations, measured distance back, perpendicular from leading edge.

Component	Full Scale Baseline Pos	NASA 10% Q5m Pos	ONERA 5.1% F1 Pos	ONERA 5.1% F1 Δ Baseline	KHI 3.23% KLWT Pos	NASA 5.2% Pos	NASA 2.7% Pos
Wing							
Up Inbd	16in	1.6in	0.6in	27%	0.5in	0.8in	0.4in
Up Midbd	12in	1.2in	0.4in	35%	0.4in	0.6in	0.3in
Up Outbd	12in	1.2in	0.2in	68%	0.4in	0.6in	0.3in
Lower	None	-	-	-	-	-	-
Fuselage							
Nose	20in	2in	1.9in	85%	0.6in	1in	0.5in
Peniche	20in	2in	-	-	-	1in	-
Nacelle							
Outer	8in	0.8in	0.3in	27%	0.3in	0.4in	0.2in
Inner	18in	1.8in	0.9in	3%	0.6in	0.9in	0.5in
Pylon							
Top	5in	0.5in	0.4in	56%	0.2in	0.3in	0.1in
Side	None	-	-	-	-	-	-
HT							
Upper	10% ch	-	10% ch		10% ch	-	10% ch
Lower	10% ch	-	10% ch		10% ch	-	10% ch

sensitivities through coordinated testing across multiple facilities and model implementations.

4.2 Model-to-Tunnel Installation Considerations and Investigations

The NASA 10%-scale model and the NASA 5.2%-scale CRM-HL model are semispan models, or half models, installed on the floor or wall of the wind tunnels that they were tested in, with external balances, outside of the model and outside of the test section. The ONERA 5.1%-scale LRM-HL model was tested with both a single-strut and three-strut installation, with the struts entering through the belly of the model in the F1. All ONERA data shown in this paper were taken with the single-strut installation, shown in Figure 2. The ONERA model with the strut installation utilized an external balance, outside of the model and outside of the test section. The KHI 3.23%-scale CRM-HL model and the NASA 2.7%-scale CRM-HL FS model were installed for testing using a sting mount, with an upper swept portion mimicking a vertical tail, with the balance internal to the model. The NASA Upper Swept Strut, shown in Figure 20 was used to install the NASA 2.7%-scale CRM-HL FS model in both NTF and ETW. The strut mimics a vertical tail on the model, but it attaches to the back end of the balance and is non-metric. The strut support structure behind the upper swept strut was different between the two tunnels, however those connections should be far enough back in the tunnel to not affect flow forward to the model.

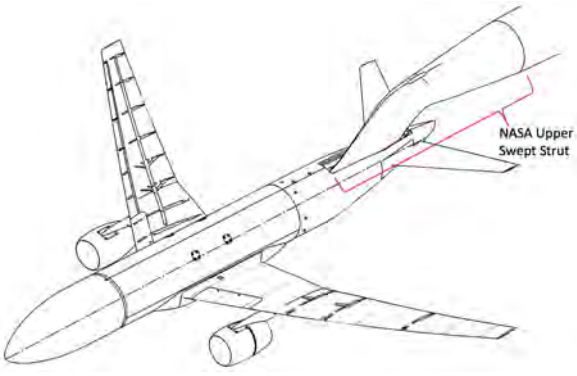


Figure 20 – Drawing of the NASA 2.7%-scale CRM-HL FS model with the NASA Upper Swept Strut.

Support system differences between semispan and full-span installations may influence spanwise loading distributions and three-dimensional flow development. Semispan models introduce wall interactions that can alter local flow structures relative to free flight or full-span configurations. Although these effects are generally small throughout the linear lift region, they can become increasingly important as the flow approaches $C_{L_{Max}}$ and separation begins to develop. Therefore extensive studies by NASA [22] [23] guided the selection of a peniche used for the NASA 5.2%-scale tests reported here to minimize the interaction between the model and the tunnel wall boundary layer. It is standard for NASA semispan models to have a peniche or standoff, a plate that follows the contours of the fuselage, attached between the floor or wall and the semispan fuselage which offsets the model from the floor or wall in an effort to extend the model out of the boundary layer. In the NWB, the peniche, or standoff, was 2.75-inches (69.9mm), with a 0.25-inch (6.4mm) gap, putting the fuselage 3-inches (76.2mm) above the tunnel floor. A brush seal was used between the peniche and the floor where the peniche overhung the turntable. For the first 14x22 entry a 1-inch (25.4mm) peniche was used, with a 0.25-inch (6.4mm) gap, setting the fuselage 1.25-inches (31.8mm) above the floor. The entire peniche fit within the bounds of the turntable, so the entire peniche to tunnel floor junction was taped. For the second 14x22 entry a 2-inch (50.8mm) peniche was used with a 0.25-inch (6.4mm) gap, placing the fuselage 2.25-inches (57.2mm) above the tunnel floor, again with the entire peniche to floor juncture taped. In the NTF a 2-inch (50.8mm) peniche was used with a 0.25-inch (6.4mm) gap, placing the fuselage 2.25-inches (57.2mm) out from the wall. A spring loaded Teflon seal was incorporated between the peniche and the tunnel wall where the peniche overhung the turntable. Data repeatability between these three tests, shown in Figure 10 indicates that the installation of the NASA 5.2%-scale SS model is consistent, and not the reason for the lower C_L on the model compared to the ONERA F1 data.

The good comparison of the upper swept strut/sting mounted KHI and NASA models at Re_C 1.1M shown in Figure 9 and the NASA 2.7%-scale tunnel-to-tunnel comparison at Re_C 1.6M shown in Figure 16 gives confidence that the installations and mountings of the models into their respective test sections were done properly.

Fouling circuits, which alert if the metric (sensed by the balance) model touches the non-metric (not sensed by the balance) support structure, were installed between the peniche and the fuselage for all testing of the NASA 5.2%-scale CRM-HL model. While the model did foul a couple of times in DLR and 14x22, no data were taken during fouling. Balance and model check loads were done prior to testing for all installations of the NASA 5.2%-scale SS model and the NASA 2.7%-scale FS CRM-HL model. All check loads were within the balance tolerances, and these check loads would detect bridging of the balance (instrumentation cables in the model pulling, causing forces on the balance) as well as other installation issues. Weight tares were done throughout testing on the NASA 5.2%-scale CRM-HL model at NTF, and for both installations of the NASA 2.7%-scale FS model which also would detect any bridging of the balance. Weight tares were not done on the floor mounted semispan models because the weight of the model does not change when pitched on the floor plane, though checks were done to assure this was the case. **The NASA team is confident that there was no fouling of the model and no bridging of the balance, giving confidence that the model to tunnel installation was not affecting the aerodynamic results.**

The NASA 5.2%-scale CRM-HL model peniche was fully taped to the 14x22 tunnel floor, so there was no flow between the peniche and the floor during testing at the 14x22, and with the good comparisons between the 14x22 data and the NWB and NTF data, confidence that there was no flow between the peniche and the tunnel translates to those tests as well. Each NASA semispan fuselage and each peniche used with the semispan models have tongue and groove or puzzle like lips, forming a labyrinth seal between the peniche (non-metric) and the fuselage (metric) to prevent airflow between the two while also keeping them far enough apart to prevent fouling [22]. A consideration for the lower C_L on the NASA 5.2%-scale model was the potential that there could be excessive flow getting around the labyrinth seal in to the fuselage cavity, causing forces on the model that would create a lower C_L. During the test at NTF cavity pressures in the fuselage were connected to the data system, and recorded and monitored. While the pressure measurements did show some flow in the fuselage cavity, the amount of flow was small. **While the flow seen inside of the NASA 5.2%-scale**

semispan fuselage cavity was measured to be small this is still something worth looking into more during future semispan testing. A run with the peniche to fuselage gap taped is planned during the next NASA 5.2%-scale installation.
The cavity where the NASA Upper Swept Strut enters the NASA 2.7%-scale fuselage was closed off with a soft bulb seal to prevent flow from the tunnel from entering the fuselage cavity while also being soft enough to not transfer any of the model load to the sting. The gap at the bulb seal was checked during each model change and six strut seal pressures were measured throughout testing to confirm that there was no flow in the cavity.

4.3 Tunnel Flow Considerations and Investigations

The tunnel environment itself represents another potential contributor to the observed differences in aerodynamic performance across the CRM-HL test campaigns. Although modern wind tunnels are carefully characterized and corrections are applied where appropriate, differences in test-section flow quality, turbulence intensity, wall boundary-layer development, and facility-specific operating conditions can influence the measured aerodynamic response, particularly near stall. The ONERA F1 tunnel, the NTF tunnel, and the ETW tunnel are pressurized tunnels. NTF and ETW closely monitor and control Mach, pressure and temperature. The KHI KLWT, the NASA 14x22, and the NWB are atmospheric wind tunnels which control Mach number, but pressure and temperature can vary based on the conditions in the external environment. The tunnel-to-tunnel and test-to-test comparisons show consistent C_L trends. Testing of the NASA 5.2% CRM-HL SS model in the NASA 14x22, in the NWB and in the NASA NTF provided comparison data from three different wind tunnels, three different balances, using three independent data reduction routines. Data repeatability between these three tests, shown in Figure 10, indicates that the difference between the NTF and F1 data is not due to non-uniform flow in the tunnels or to fluctuating tunnel flow conditions.
Boundary layer effects were considered as potentially having an effect on the semispan force and moment data. A flow rake was installed on the NTF wall ahead of the NASA 5.2%-scale SS model for a set of of runs at varying Reynolds numbers in air during NTF Test 237. For the full range of Reynolds numbers checked, the pressure rake showed the measured pressure reaching free-stream pressure 2 inches (50 mm) off the wall, which was the peniche height used for that test, placing the fuselage .25 inches (6.4mm) outside of the boundary layer. The NASA 14x22 wind tunnel did utilize a boundary layer removal system in front of the model, the use of which was shown to have an effect on the model forces [6] and was used throughout testing of the NASA 5.2%-scale CRM-HL model in the 14x22 tunnel.
As noted previously, the test of the ONERA 5.1%-scale FS LRM-HL model in the ONERA F1 and the test of the NASA 2.7%-scale CRM-HL model in the ETW used continuous data collection, while the other CRM-HL test campaigns used pitch pause data collection at discrete alphas. Flow attachment on a model can differ at a given model alpha based on how the model alpha was approached, and was therefore worth investigating. Figure 21 shows comparisons of continuous data runs with pitch pause data runs on the same models at the same conditions in NTF. No changes are seen in the force and moment data with the different collection methods.

4.4 Data Reduction Considerations and Investigations

Wind tunnels have standard procedures, best practices, and data verification processes to ensure that data are being collected and computed properly. The NASA 5.2%-scale CRM-HL model was tested at three wind tunnels, NWB, 14x22 and NTF, all using independent data reduction programs, and independent instrumentation. Standard data reduction routines were used in all three tunnels, with no special non-standard corrections applied to the data. Wall corrections were applied to the data in all three tunnels, however the NTF 5.2%-scale Test 237 data does not have final Transonic Wall Interference Correction System (TWICS) wall corrections applied, only classical wall corrections [24], and is therefore still considered preliminary data. Figure 10 is a force and moment plot of the NASA 5.2%-scale CRM-HL, Landing - Nacelle On, Mach 0.2, Re_C 1.6M repeat at the three different tunnels. The pitching moment coefficient at NTF is slightly lower than it is at the other tunnels, but the data does repeat well between the three tunnels. **The good repeatability in force and moment data for the NASA 5.2%-scale CRM-HL in three different tunnels, with independent data reduction**

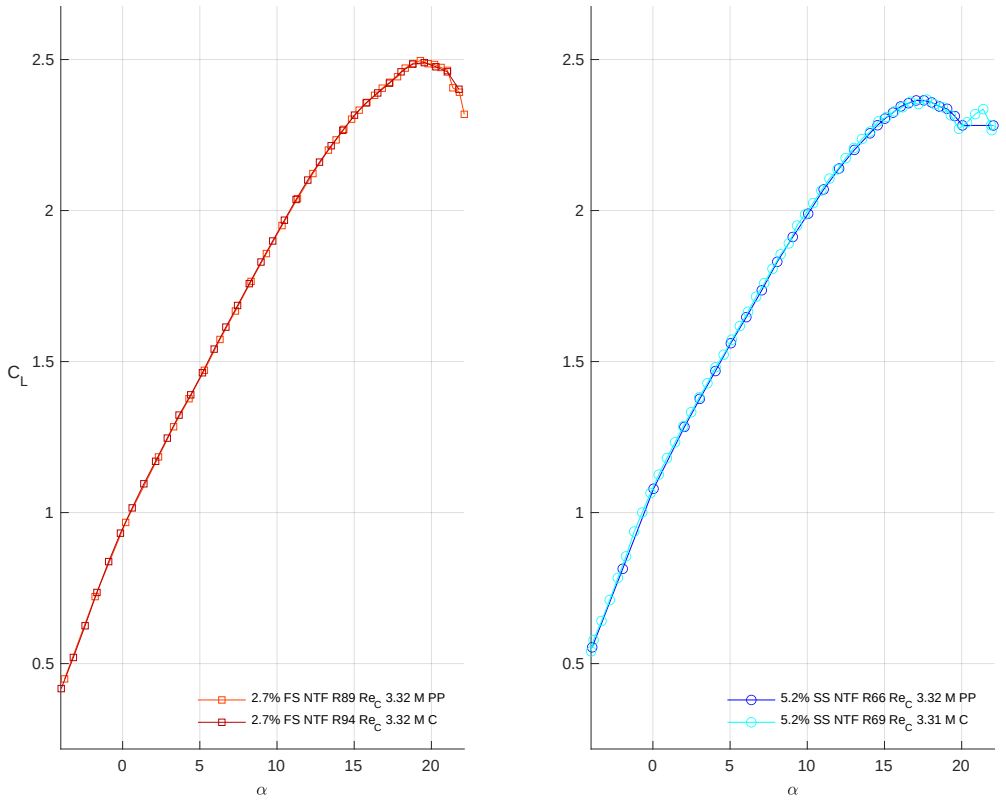


Figure 21 – C_L vs. α, pitch pause vs. continuous runs in the NTF, NASA CRM-HL models in the Landing - Nacelle configuration, Mach 0.20, Re_C 3.32M.

programs, independent setup and independent instrumentation indicates that the C_L is not lower for the NASA model because of a data reduction error.
The three tests of the two strut mounted models, KHI and NASA FS in NTF and ETW, applied standard tunnel calibration corrections to tunnel Mach and pressure, model blockage corrections and buoyancy, flow angularity corrections and wall corrections. No model support corrections were applied and no special non-standard corrections were applied to these data sets. The differences seen in the NASA 2.7%-scale tunnel-to-tunnel force and moment comparisons at higher Re_C seen in Figures 15 and 16 will be investigated once ETW provides final data. ONERA F1 corrections applied to the data were wall interference corrections based on linearized potential theory and support corrections based on a previous test campaign in which a similar model was tested with and without a dummy strut. **Further examination of correction methods across all tunnel supporting CRM-HL activities could provide valuable insights into the observed differences in force and moment values.**

5. Concluding Remarks

The CRM-HL ecosystem continues to evolve as a global benchmark for high-lift aerodynamics, integrating standardized geometry, modular design, and coordinated wind tunnel campaigns to advance CFD validation and simulation-driven certification. The inclusion of the 2025–2026 NTF Test 240 phases-covering both air-only and cryogenic entries marks a critical expansion of the ecosystem's Reynolds-number envelope and configuration diversity. These tests provide unprecedented opportunities to study icing effects, validate turbulence and transition models under flight conditions, and strengthen cross-scale comparisons with prior campaigns. By continuing to test the CRM-HL ecosystem models, extending the well defined dataset, the CRM-HL ecosystem ensures that future certification workflows will rely on robust, physics-based predictions, reducing dependence on costly physical testing and costly CFD simulations, and accelerating innovation in commercial transport design.
The consistent tunnel-to-tunnel and test-to-test comparisons with noted C_L magnitude variations resulted in numerous investigations being conducted to find the source or sources of the differences.

Known model OML differences and semispan effects are likely contributors to the C_L magnitude variation, and inaccurate as-built wind tunnel models, tunnel installation issues, non-uniform tunnel flow, tunnel flow conditions, and continuous vs. pitch pause data collection operation are likely not contributors. Planned future investigations, noted above, include a full scan of the NASA 2.7%-scale model, a wing deformation study in CFD, a semispan test of the NASA 2.7%-scale FS model in NTF, a trip dot study during the cryogenic entry of the NASA 2.7%-scale FS model in the NTF, and a more in depth look at the comparison data between NTF and ETW once ETW provides final data. A study of wall correction methodology between tunnels and tunnel specific data correction magnitudes would be of interest and could provide valuable insights into the observed differences in force and moment values. A deeper look into wing pressures measured on the models during each test entry is in work and will provide valuable information.

The ability to compare results across multiple wind tunnel campaigns is fundamental to the CRM-HL ecosystem's mission of achieving certification-level confidence in predictive methods. These comparisons provide a rigorous framework for identifying facility-specific biases, geometric sensitivities, and Reynolds number effects that influence aerodynamic performance near stall. By analyzing trends in lift, drag, and pitching moment across different scales, configurations, and test environments, researchers can isolate the impact of design variations—such as bracket geometry, sealing details, and instrumentation allowances—from true aerodynamic phenomena.

The CRM-HL ecosystem has evolved beyond a traditional wind-tunnel test program into a comprehensive validation framework for high-lift aerodynamics. Through coordinated testing across multiple facilities, Reynolds numbers, model scales, and support-system implementations, the ecosystem provides a unique opportunity to quantify physical, geometric, and facility related sources of variability. The obtained data are directly enabling verification and validation for next-generation CFD methods.

In parallel with the experimental efforts, NASA has established the Data Organization and Retrieval Application (DORA) [25] as a centralized repository for test data, metadata, geometry definitions, documentation, with the plan of hosting future computational results. By providing a common environment for data preservation, organization, and sharing across the ecosystem partners, DORA helps ensure that the value of individual test campaigns extends beyond their original objectives. This centralized data infrastructure supports reproducibility, cross-campaign analyses, and long-term verification and validation activities while enabling future researchers to benefit from the full breadth of CRM-HL experimental and computational datasets.

6. Contact Author Email Address

The contact author email address is courtney.s.winski@nasa.gov.

7. Copyright Statement

The authors confirm that they, and/or their company or organization, hold copyright on all of the original material included in this paper. The authors also confirm that they have obtained permission, from the copyright holder of any third party material included in this paper, to publish it as part of their paper. The authors confirm that they give permission, or have obtained permission from the copyright holder of this paper, for the publication and distribution of this paper as part of the ICAS proceedings or as individual off-prints from the proceedings.

8. Acknowledgments

This research is sponsored by the NASA Transformational Tools and Technologies (TTT) Project of the Transformative Aeronautics Concepts Program (TACP) under the Aeronautics Research Mission Directorate (ARMD).

References

[1] Doug S. Lacy and Anthony J. Sclafani. Development of the high lift common research model (HL-CRM): A representative high lift configuration for transonic transports. In *2016 AIAA SciTech Forum*, 2016-0308, SanDiego, CA, Jan. 2016. AIAA.

[2] Douglas Lacy and Adam M. Clark. Definition of initial landing and takeoff reference configurations for the high lift common research model (CRM-HL). In *AIAA Aviation Forum 2020*, 2020-2771, Virtual Event, June 2020. AIAA.

[3] Ashley Evans, Doug Lacy, Ian Smith, and Melissa Rivers. Test summary of the NASA semi-span high-lift common research model at the QinetiQ 5-metre low-speed wind tunnel. In *2020 AIAA Aviation Forum*, 2020-2770, Virtual Event, 2020/06 2020. AIAA.

[4] Sylvain Mounton, Grégoire Charpentier, and Annabelle Lorenski. Test summary of the full span high lift common research model at the ONERA F1 pressurized low speed wind tunnel. In *2023 AIAA SciTech Forum*, 2023-0823, San Diego, California, 2023/01 2023. AIAA.

[5] Sylvain Mounton, Grégoire Charpentier, and Annabelle Lorenski. Testing the full span high lift common research model at the ONERA F1 pressurized low speed wind tunnel. In *AIAA Aviation Forum and Ascend 2024*, 2024-3512, Las Vegan, Nevada, July 2024. AIAA.

[6] Courtney S. Winski, Sarah L. Langston, and S. Melissa Rivers. NASA 5.2% semispan high lift common research model wind tunnel test at the 14- by 22-foot subsonic wind tunnel. In *2025 AIAA SciTech Forum*, 2025-0249, Orlando Florida, Jan. 2025. AIAA.

[7] Takahiro Hashioka, Yoshiki Murahashi, Hidemasa Yasuda, Yuta Sawaki, Sho Onda, Yuta Tsuchimoto, Yusuke Nishizaki, Wataru Suzuki, and Takeo Kawamura. Test summary of the full-span high-lift common research model at khi aero-acoustic low-speed wind tunnel. In *34th Congress of the International Council of the Aeronautical Sciences*, 2024-1215, Florence, Italy, Sept. 2024. ICAS.

[8] Sven Puelm, Florian N. Schmidt, Ralf Rudnik, and Courtney S. Winski. Low-speed testing of the 5.2% semi-span CRM-HL in the DNW-NWB wind tunnel. In *2024 AIAA Aviation Forum*, 2024-3516, Las Vegas, Nevada, July 2024. AIAA.

[9] Sven Puelm, Florian N. Schmidt, Ralf Rudnik, Moritz Schmidt, and Johannes Wolff. Low-speed testing of variations of the 5.2% CRM-HL with an UHBR nacelle and a krueger flap in the DNW-NWB wind tunnel. In *AIAA SciTech 2025*, 2025-0023, Orlando Florida, 01 2025. AIAA.

[10] Courtney S. Winski, Sarah Langston, Melissa Rivers, and Miranda Ertsgaard. NASA 5.2%-scale semispan high lift common research model (CRM-HL) high reynolds number wind tunnel test in the national transonic facility (NTF). In *2025 AIAA Aviation Forum*, 2025-3461, Las Vegas, Nevada, July 2025. AIAA.

[11] Sarah L. Langston, Courtney S. Winski, and S. Melissa Rivers. Reynolds number effects on a 5.2%-scale high lift common research model. In *2025 AIAA SciTech Forum*, 2025-1514, Orlando Florida, Jan. 2025. AIAA.

[12] Sarah Langston, Courtney S. Winski, and Melissa Rivers. Reynolds number effects on the surface pressures on a 5.2%-scale high lift common research model. In *2025 AIAA Aviation Forum*, 2025-3462, Las Vegas, Nevada, July 2025. AIAA.

[13] Simon Prince, David MacManus, Davide Di Pasquale, Abhay Vincent, Ankit Sharma, Steven Daniels, Kolleen K. Hood, Sean Ali, Soroush Yazdani, Ashley Evans, Neville Koh, Aleesandra Court, Farshad Soleimaninia, Melissa B. Rivers, Courtney Spells Winski, Ozoroski Thomas A, Paul White, Dietmar Meißner, James Brown, Ellliot Kane, Stuart Gates, Matthias Schulz, Constantine Jux, and Guido Diez. Icing effect experiments on the NASA high-lift common research model. In *35th Congress of the International Council of the Aeronautical Sciences*, 2026-TBD, Sydney, Australia, Sept. 2026. ICAS.

[14] C. L. Rumsey, J. P. Slotnick, and C. D. Woeber. Hlpw-4/gmgw-3: Overview and workshop summary. In *AIAA Aviation Forum*, 2022-3295, Chicago, Illinois, June 2022. AIAA.

[15] Florian N. Schmidt and Jochen Wild. Design of an UHBR through flow nacelle and a krueger flap for the CRM-HL. In *AIAA SciTech 2024*, 2024-285, Orlando Florida, 01 2024. AIAA.

[16] Andy P. Broeren, Thomas A. Ozoroski, Christopher E. Porter, and Kolleen K. Hood. Aerodynamic effect of artificial ice shapes on the 5.2% scale semispan high-lift common research model in the NASA national transonic facility. In *2025 AIAA Aviation Forum*, 2025-3463, Las Vegas, Nevada, July 2025. AIAA.

[17] Miranda L. Ertsgaard and Courtney S. Winski. Development of NASA 5.2%-scale semispan high lift common research. In *2025 AIAA SciTech Forum*, 2025-1127, Orlando Florida, Jan. 2025. AIAA.

[18] NASA. CRM-HL reference geometry files. Webpage, 2023.

[19] Miranda Ertsgaard and Courtney S. Winski. Development of NASA 2.7% semispan and full span high lift common research models (CRM-HL). In *2025 AIAA Aviation Forum*, 2025-3460, Las Vegas, Nevada, July 2025. AIAA.

[20] Hexagon. Hexagon absolute scanner as1. Website, 2025.

[21] Timothy Fahringer, Loc Tran, and David Keck. Development of the model deformation system at the national transonic facility. In *AIAA SciTech Forum 2024*, 2024-2573, Orlando, FL, 01 2024. AIAA.

[22] G. Gatlin, P. Parker, and L. Owens. Development of a semi-span test capability at the national transonic

facility. In *AIAA Aerospace Sciences Meeting 2001*, 2001-0759, Reno, NV, 01 2001. AIAA.

[23] Gregory Gatlin, William Tomek, Francis Payne, and Robert Griffiths. Recent improvements in semi-span testing at the national transonic facility (invited). In *44th AIAA Aerospace Sciences Meeting and Exhibit*, 2006-508. AIAA, 2020/06 2006.

[24] Venkit Iyer. A wall correction program based on classical methods for the national transonic facility (solid wall or slotted wall) and the 14x22-ft subsonic tunnel at NASA LaRC. CR 2004-213261, NASA, Oct. 2004.

[25] NASA. DORA, https://crm-hl.aetc.appdat.jsc.nasa.gov/. Webpage, 2026.